LABORATORI NAZIONALI DI FRASCATI

SIS-Pubblicazioni

LNF-00/026(P)
20 Ottobre 2000

UWThPh-2000-40

$K \to \pi\pi e^+e^-$ decays and chiral low-energy constants*

Hannes Pichl

INFN, Laboratori Nazionali di Frascati,
I-00044 Frascati, Italy
and
Institut für Theoretische Physik, Universität Wien,
A-1090 Wien, Austria

Abstract

In this paper the branching ratios of the measured decay $K_L \to \pi^+\pi^- e^+e^-$ and of the still unmeasured decay $K^+ \to \pi^+\pi^0 e^+e^-$ are calculated to next-to-leading order in Chiral Perturbation Theory (CHPT). Recent experimental results are used to determine two possible values of the combination $(N_{16}^r - N_{17})$ of weak low-energy couplings (LEC) from the $\mathcal{O}(p^4)$ chiral Lagrangian. Furthermore, the obtained values are compared to theoretical models of weak counterterm couplings to distinguish between the two possibilities. Using the favoured value of the combination $(N_{16}^r - N_{17})$ and taking into account additional assumptions suggested by these models, one can predict the branching ratio of the second decay as a function of the numerically unknown combination $(N_{14}^r + 2N_{15}^r)$ of weak low-energy couplings. Finally, making use of a particular model for the individual LECs, one predicts the decay width of the K^+ decay in question.

*Work supported in part by TMR, EC-Contract No. ERBFMRX-CT980169 (EURODAΦNE)

PACS.: 12.39.Fe; 13.25. Es

Submitted to European Physical Journal C

1 Introduction

During the last years, there has been a lot of theoretical and experimental interest in the decay of the K_L into a pair of charged pions and a pair of leptons. This interest focused on the decay width itself [1, 2, 3, 4, 5, 6, 7] and on the possibility of constructing CP-violating observables [1, 2, 3, 4, 8, 9, 10] as well as on other related topics [11, 12].

From the experimental analysis of the corresponding radiative decay, it was found that the decay amplitude consists of a bremsstrahlung component and a direct emission part. The contribution due to bremsstrahlung is, of course, given via Low's theorem by the amplitude of the decay $K_L \to \pi^+\pi^-$. This amplitude is mainly due to the K_1^0 admixture, which allows for this decay. As a consequence, the final state of the radiative decay can be found to be in CP-even as well as CP-odd configurations. Hence, in principle, there is interference between the CP-conserving parts of the direct emission amplitude and the CP-violating bremsstrahlung amplitude. But as long as the polarization of the on-shell photon is not measured, this interference does not occur. This is the reason why one looks directly to the decay with the lepton pair, since the angle between the two planes spanned by the pions and leptons, respectively, can be used to construct a CP-violating observable [1, 2, 3, 4, 8].

In this paper, I will not focus especially on the CP-violating aspects of this decay. I calculate the decay amplitude in CHPT up to $\mathcal{O}(p^4)$, and I will use the most recent available data from experiments [9, 13] (which were mostly dedicated to the study of possible CP-violating effects) to derive numerical values for the remaining unknown combination of weak counterterm couplings (LECs) $(N_{16}^r - N_{17})$ of the $\mathcal{O}(p^4)$ chiral Lagrangian for this decay (see Section 2). Until now, theory predictions can only be compared with the BR over the entire phase space, which makes it impossible to extract precise values for the combination of LECs. Furthermore, it is not possible to determine this value unambiguously from experiment, therefore one has to turn to theoretical models and their predictions for these couplings to distinguish the favoured value.

Once the numerical value of this particular combination is fixed, I use it as an input together with additional assumptions about the weak LEC N_{17} for the second non-leptonic decay which I will discuss in this paper: $K^+ \to \pi^+\pi^0 e^+ e^-$. If we use new data from the corresponding radiative decay $K^+ \to \pi^+\pi^0\gamma$ [14], we can give the magnetic amplitude of $K^+ \to \pi^+\pi^0 e^+ e^-$ without any unknown parameter (at $\mathcal{O}(p^4)$). Thus, the obtained branching ratio is predicted as a function of only one unknown combination of low energy couplings: $(N_{14}^r + 2N_{15}^r)$.

2 Effective chiral Lagrangians

Chiral Perturbation Theory (CHPT) [15, 16] is the ideally suited framework to discuss these processes. It is the low-energy realization of the Standard Model which respects the approximate chiral symmetry of the light quark sector. In fact, the demand of invariance under chiral rotations (in our case, these are $SU(3)$ rotations) allows one to write down the most general effective Lagrangian of strong interactions amongst the light pseudoscalar meson octet. The approximate chiral symmetry $SU(3)_L \times SU(3)_R$ seems to be realized à la Nambu-Goldstone, which means that it is spontaneously broken to the well-known $SU(3)_V$. The breakdown of the symmetry gives rise to eight nearly massless would-be Goldstone bosons because there are eight broken axial generators. According to Goldstone's theorem, the quantum numbers of these particles are fixed by the quantum numbers of the broken generators, thus one identifies the light mesons with these particles. In the scheme of Gasser and Leutwyler, the most general $\mathcal{O}(p^2)$ Lagrangian which includes strong, electromagnetic and also semileptonic weak interactions reads as follows:

$$\mathcal{L}_2 = \frac{F^2}{4}\langle D_\mu U D^\mu U^\dagger + \chi U^\dagger + \chi^\dagger U\rangle, \tag{1}$$

where $D_\mu U$ is the covariant derivative with respect to external, non-propagating fields. If we specialize to the case of external photons,

$$D_\mu U = \partial_\mu U + ieA_\mu[Q,U], \quad Q = \frac{1}{3}\mathrm{diag}(2,-1,-1), \tag{2}$$

where Q is the quark charge matrix for u, d, s. U is a 3×3 unitary matrix which has to be expanded to the relevant order in Φ:

$$U(\Phi) = e^{i\sqrt{2}\Phi/F}, \tag{3}$$

where the mesons are collected in the Φ matrix:

$$\Phi = \frac{1}{\sqrt{2}}\lambda_a\phi^a = \begin{pmatrix} \pi^0/\sqrt{2}+\eta_8/\sqrt{6} & \pi^+ & K^+ \\ \pi^- & -\pi^0/\sqrt{2}+\eta_8/\sqrt{6} & K^0 \\ K^- & \bar{K}^0 & -2\eta_8/\sqrt{6} \end{pmatrix}. \tag{4}$$

F equals to lowest order the pion decay constant, $F_\pi = 92.4$ MeV. In general, χ contains external scalar and pseudoscalar matrix-valued fields, but here it is proportional to the quark mass matrix. In this way, explicit chiral symmetry breaking can be incorporated in the effective Lagrangians in a very elegant way:

$$\chi = 2B_0\mathrm{diag}(m_u, m_d, m_s). \tag{5}$$

B_0 is related to the order parameter of the spontaneous breakdown of the chiral symmetry, the quark condensate. It will not appear explicitly because it can be absorbed in the meson masses.

For the calculation of non-leptonic kaon decays, we also need an effective Lagrangian which describes the weak interactions of the mesons. The effective weak Lagrangian is not invariant under chiral rotations, hence the construction of it follows a different approach. Starting from an effective strangeness-changing $\Delta S = 1$ four-quark Hamiltonian, one writes down a hadronically realized Lagrangian which transforms in the same way under $SU(3)_L \times SU(3)_R$ as this Hamiltonian. To lowest order, the needed Lagrangian is found to be this expression:

$$\mathcal{L}_2^{\Delta S=1} = G_8 \langle \lambda L_\mu L^\mu \rangle + G_{27} \langle L_{\mu 23} L_{11}^\mu + \frac{2}{3} L_{\mu 21} L_{13}^\mu \rangle + h.c., \tag{6}$$

where $\lambda = (\lambda_6 - i\lambda_7)/2$ projects out the correct octet quantum numbers and $L_\mu = iF^2 U^\dagger D_\mu U$ is the hadronic left-chiral current in analogy to the left-chiral quark current at the level of the effective Hamiltonian. The two couplings G_8 and G_{27} have to be obtained from experiment and the determination of these couplings involves some subtleties. In principle, the couplings are obtained from $K \to \pi\pi$ decays. Comparison with the leading order $\mathcal{O}(p^2)$ calculations yields $|G_8| \simeq 9.1 \cdot 10^{-6}\text{GeV}^{-2}$ and $G_{27}/G_8 \simeq 1/18$, where the ratio of the two couplings introduces considerable uncertainties when the 27-plet coupling enters the game. Due to the smallness of the 27-plet coupling, one can usually neglect this part of the Lagrangian, unless the octet contribution vanishes. Then the 27-plet contribution has to be taken into account (see Section 3.2). In Ref. [17], the relevant $K \to \pi\pi$ decays were analyzed up to $\mathcal{O}(p^4)$ and it was found that these additional corrections contribute to G_8 with about 30%, whereas the G_{27} coupling is only modified by a few percent. In fact, if one takes into account these p^4 corrections, the coupling $|G_8|$ appearing in (6) should be about $6.4 \cdot 10^{-6}\text{GeV}^{-2}$. We will come back to this in Section 3.1.

According to the chiral counting rules, these Lagrangians allow us to calculate tree-level amplitudes as well as one-loop diagrams which usually introduce divergences. Loop diagrams are chirally counted as $\mathcal{O}(p^4)$, thus one also has to consider the most general $\mathcal{O}(p^4)$ interactions to remove these divergences and to include further finite local corrections to this order, e.g., new interactions which come from the chiral anomaly.

The most general strong Lagrangian of fourth order, C, P, Lorentz and chiral invariant, was again given by Gasser and Leutwyler [16]. There is only one term in this Lagrangian that contributes to the final results in this work:

$$\mathcal{L}_4 = -iL_9 \langle F_R^{\mu\nu} D_\mu U D_\nu U^\dagger + F_L^{\mu\nu} D_\mu U^\dagger D_\nu U \rangle. \tag{7}$$

In the case of external photons, the $F^{\mu\nu}_{L,R}$ tensors are proportional to the ordinary electromagnetic field strength tensor:

$$F^{\mu\nu}_L = -eQF^{\mu\nu} = F^{\mu\nu}_R, \quad F^{\mu\nu} = \partial_\mu A_\nu - \partial_\nu A_\mu. \tag{8}$$

Every new term in the strong Lagrangian of fourth order is furnished with an a priori unknown coupling (LEC) [16]. Since all divergences appear as local polynomials, one can absorb the divergent parts of the amplitude in the LECs. The general structure of a LEC is as follows:

$$L_i = L^r_i(\mu) + \Gamma_i \frac{\mu^{d-4}}{16\pi^2}\left\{\frac{1}{d-4} - \frac{1}{2}(\ln 4\pi + 1 - \gamma_E)\right\}, \tag{9}$$

where $\gamma_E = 0.5772157$ is the Euler-Mascheroni constant. This is also true for weak LECs. The coefficients Γ_i arise from the one-loop generating functional: $\Gamma_9 = \frac{1}{4}$. Because of the regularization procedure, the measurable couplings L^r_i become scale dependent. In the end, this scale dependence is compensated by the scale dependent parts of loop diagrams. One should note that the chiral subtraction prescription differs from the usual modified MS prescription.

The new octet weak interactions are organized like this [18, 19]:

$$\mathcal{L}_4^{\Delta S=1} = G_8 F^2 \sum_i N_i W_i. \tag{10}$$

For the non-leptonic kaon decays under consideration, only $W_{14}, W_{15}, W_{16}, W_{17}$ and $W_{28}, W_{29}, W_{30}, W_{31}$ contribute; they are listed explicitly:

$$\begin{aligned}
W_{14} &= i\langle\lambda\{F^{\mu\nu}_L + U^\dagger F^{\mu\nu}_R U, D_\mu U^\dagger D_\nu U\}\rangle,\\
W_{15} &= i\langle\lambda D_\mu U^\dagger (U F^{\mu\nu}_L U^\dagger + F^{\mu\nu}_R) D_\nu\rangle,\\
W_{16} &= i\langle\lambda\{F^{\mu\nu}_L - U^\dagger F^{\mu\nu}_R U, D_\mu U^\dagger D_\nu U\}\rangle,\\
W_{17} &= i\langle\lambda D_\mu U^\dagger (U F^{\mu\nu}_L U^\dagger - F^{\mu\nu}_R) D_\nu U\rangle.
\end{aligned} \tag{11}$$

The magnetic terms are

$$\begin{aligned}
W_{28} &= i\epsilon_{\mu\nu\rho\sigma}\langle\lambda D^\mu U^\dagger U\rangle\langle U^\dagger D^\nu U D^\rho U^\dagger D^\sigma U\rangle,\\
W_{29} &= 2\langle\lambda[U^\dagger \tilde{F}^{\mu\nu}_R U, D_\mu U^\dagger D_\nu U]\rangle,\\
W_{30} &= \langle\lambda U^\dagger D_\mu U\rangle\langle(\tilde{F}^{\mu\nu}_L + U^\dagger \tilde{F}^{\mu\nu}_R U) D_\nu U^\dagger U\rangle,\\
W_{31} &= \langle\lambda U^\dagger D_\mu U\rangle\langle(\tilde{F}^{\mu\nu}_R - U^\dagger \tilde{F}^{\mu\nu}_R U) D_\nu U^\dagger U\rangle,
\end{aligned} \tag{12}$$

with $\tilde{F}^{\mu\nu}_{L,R}$ the dual tensor of (8), $\tilde{F}^{\mu\nu}_{L,R} = \epsilon^{\mu\nu\rho\sigma} F_{\rho\sigma L,R}$. Finally, we introduce a Lagrangian which accounts for reducible diagrams with a WZW-vertex and an $\mathcal{O}(p^2)$ $\Delta S = 1$ vertex. It only contributes to the K^+ decay and is simply given by [20, 21]

$$\mathcal{L}_{an}^{\Delta S=1} = \frac{ieG_8}{8\pi^2 F}\tilde{F}^{\mu\nu}\partial_\mu\pi^0 K^+ \overleftrightarrow{D}_\nu \pi^-. \tag{13}$$

$\tilde{F}^{\mu\nu}$ is the dual of the ordinary electromagnetic field strength tensor (8), $\tilde{F}^{\mu\nu} = \epsilon^{\mu\nu\rho\sigma}F_{\rho\sigma}$, and the covariant derivative is the usual QED derivative.

3 Amplitudes

For both decays, the general form of the invariant amplitude due to covariance is

$$\mathcal{A} = \frac{e}{q^2}V_\mu \bar{u}(k_-)\gamma^\mu v(k_+), \tag{14}$$

where $q = k_- + k_+$ is the momentum of the virtual photon, k_- and k_+ are the momenta of the electron and positron, respectively. iV_μ is the generic weak $K\pi\pi(\gamma^\star)$ vertex, calculated in CHPT. It is decomposed in an electric and a magnetic part

$$V_\mu = \mathcal{F}_1 p_{1\mu} + \mathcal{F}_2 p_{2\mu} + \mathcal{M}\epsilon_{\mu\nu\rho\sigma}p_1^\nu p_2^\rho q^\sigma, \tag{15}$$

where p_1 and p_2 are the outgoing momenta of the π^+ and $\pi^-(\pi^0)$ and $\mathcal{F}_1$, $\mathcal{F}_2$, $\mathcal{M}$ are form factors containing the dynamics of the two processes. A separate term with the photon momentum vanishes because of the Dirac equation. The form factors are constants or scalar functions of various products of the involved momenta.

3.1 $K_L \to \pi^+\pi^-\gamma^\star$ Amplitudes

This decay had already been considered in the framework of CHPT in [3]. These authors used a different basis of counterterms (this change of basis is only valid as long as one is only interested in photons) and a different approximation of the magnetic part of the amplitude which does not take into account any energy dependence. The present calculation considers this energy dependent part [9], too, and serves as a check on their results. For this decay, I assume strong isospin conservation, i.e., the up and the down quark have equal masses. Hence, the Gell-Mann-Okubo mass relation holds and we only have to deal with two independent masses: $3m_\eta^2 = 4m_K^2 - m_\pi^2$. Moreover, I will neglect the K_1^0 admixture in the amplitudes of chiral order p^4. I use the following definitions: $K_L = K_2^0 + \epsilon K_1^0$, where $CP|K_2^0\rangle = -|K_2^0\rangle$ and $CP|K_1^0\rangle = +|K_1^0\rangle$. K_2^0 as well as K_1^0 are defined as hermitian fields. Their relations with the strangeness eigenstates K^0 and $\bar{K}^0$ are the following:

$$\begin{aligned} K_2^0 &= \frac{1}{\sqrt{2}}(K^0 + \bar{K}^0), \\ K_1^0 &= \frac{i}{\sqrt{2}}(\bar{K}^0 - K^0). \end{aligned} \tag{16}$$

This implies that $\mathcal{A}(K^0 \to \pi\pi) = \frac{i}{\sqrt{2}}\mathcal{A}(K_1^0 \to \pi\pi)$, and equally for $\bar{K}^0$. Therefore, the present tree-level amplitude for an external K_1^0 is multiplied by an additional

factor of i compared to the tree-level amplitude in Ref. [3].

The tree-level amplitude is entirely due to the K_1^0 admixture, since we do not take into account sources of direct CP-violation. As a consequence, the tree-level contribution is rather suppressed, especially when compared to the K^+ decay.

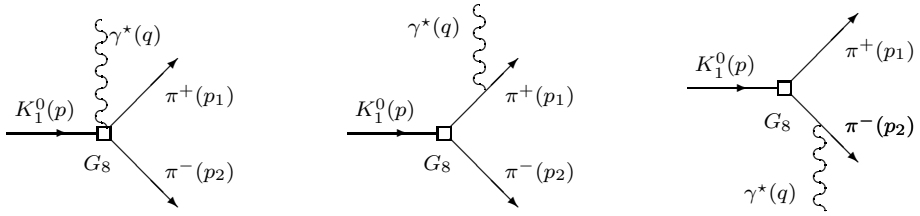

Figure 1: Tree-level diagrams for $K_L \to \pi^+\pi^-\gamma^\star$. At tree level, the K_L transition is entirely due to K_1^0 admixture.

From Figure 1 one obtains this result for the tree level:

$$\mathcal{F}_1^{Lt} = -i\epsilon\frac{4eG_8F}{2qp_1+q^2}(m_K^2-m_\pi^2), \quad \mathcal{F}_2^{Lt} = i\epsilon\frac{4eG_8F}{2qp_2+q^2}(m_K^2-m_\pi^2), \tag{17}$$

where $\epsilon \simeq 2.27\cdot 10^{-3}e^{i44^o}$ is the parameter of indirect CP-violation. In the following, we do not take into account $\mathcal{O}(p^4)$ corrections proportional to ϵ to the electric from factors. As mentioned in Section 2, a value of $G_8 \simeq 9.1\cdot 10^{-6}\text{GeV}^{-2}$ already amounts to a renormalization by $\mathcal{O}(p^4)$ contributions. Since the bremsstrahlung approximation of $K_1^0 \to \pi^+\pi^-\gamma^\star$ works very well for 'small' photon momenta (to be justified in Section 4.2), there is no need to consider next-to-leading order corrections proportional to ϵ. Using the larger value of G_8 for $\mathcal{O}(p^4)$ contributions to the electric form factors introduces an error of $\mathcal{O}(p^6)$, which we do not consider.

The magnetic form factor can only arise through the four weak counterterms $W_{28},\ldots,W_{31}$ and it is in fact a result of the chiral anomaly. It is necessarily finite and does not have any energy dependence at this order. CHPT generates the following direct emission magnetic form factor:

$$\begin{aligned}\mathcal{M}^L &= \frac{-16eG_8}{F}(N_{29}+N_{31}) \\ &= \frac{-eG_8}{2\pi^2F}(a_2+2a_4),\end{aligned} \tag{18}$$

where I have used the notation of Ref. [20, 21] in line two. Unfortunately, the magnetic LECs are still unknown, too, and experiments show a large sensitivity

of the magnetic amplitude on the energy of the emitted photon. Therefore, I will use the experimental results of [9] (rather than the old results of the experiment by Ramberg et al., [22]) to estimate the magnetic contribution. The authors of Ref. [9] use the papers by Sehgal et al. [1, 2] as the theoretical background to model their Monte Carlo, but additionally introduce an energy dependence in the magnetic amplitude through a form factor that involves a kind of a ρ propagator:

$$\mathcal{M}^L = e|f_s|\frac{\tilde{g}_{M1}}{m_K^4}\mathcal{W} = e|f_s|\frac{\tilde{g}_{M1}}{m_K^4}[1 + \frac{a_1/a_2}{(m_\rho^2 - m_K^2) + 2m_K E_\gamma^\star}]. \tag{19}$$

This ansatz cannot be compared directly to the one in [1, 2, 3, 4, 8]. According to [9], one rather has to identify the average of $\tilde{g}_{M1}\mathcal{W}$ over the $E_\gamma^\star$ range with the magnetic coupling in Ref. [1, 2]. $|f_s| \simeq 3.9 \cdot 10^{-4}$ is a coupling constant, and the experiment [9] gives us $|\tilde{g}_{M1}| = 1.35^{+0.20}_{-0.17}(\text{stat.}) \pm 0.04(\text{syst.})$ and $a_1/a_2 = -0.720 \pm 0.028(\text{stat.}) \pm 0.009(\text{syst.})$ GeV^2. (a_1 and a_2 in the fraction above are not the same as the LECs a_2 and a_4 of (18).) These numbers were obtained from the entire KTeV 1997 data set of more than 1811 events above background. In fact, it is also this data set and this parametrization that were used to extract the most recent value of the branching ratio of $K_L \to \pi^+\pi^- e^+ e^-$ [13]. Additionally, the fraction a_1/a_2 was found from the corresponding radiative decay $K_L \to \pi^+\pi^-\gamma$ to be $-0.729 \pm 0.026(\text{stat.}) \pm 0.015(\text{syst.})$ GeV^2 [10], which is clearly in perfect agreement. The errors of these quantities are the sources of by far the most important contribution to the uncertainties in the extraction of the LEC combination $(N_{16}^r - N_{17})$.

The electric form factors at $\mathcal{O}(p^4)$ show the pleasant feature that one can obtain the form factor $\mathcal{F}_2^L$ from the expression for $\mathcal{F}_1^L$ by simply exchanging the pion momenta p_1 and p_2 because of CP. At this order, there is no change of sign like at the tree level, since we concentrate on the CP-conserving part of the decay.

First, I will consider the impact of strong loops and of the vertex from the strong next-to-leading order counterterm (7) on the electric amplitude. The complete strong $\mathcal{O}(p^4)$ contribution to the form factors is obtained in two steps.

The starting point for this part of the analysis of the decay amplitude is again Figure 1, where one replaces K_1^0 with K_2^0. It is clear that strong $\mathcal{O}(p^4)$ corrections can only appear as loop or counterterm insertions in mesonic lines in the diagrams of Figure 1. Second, it turns out that only two types of strong insertions contribute to the electric form factors.

The first kind of insertions is shown in Figure 2. One inserts a loop in any external line and appends a virtual photon on the strong vertex or on a charged loop particle (Figure 2a). The insertion of the strong counterterm vertex derived from (7) concerns only the external pions (Figure 2b). The second class of insertions only refers to the kaon line in Figure 1. It is given by the diagrams in Figure 3 (neutral kaonic charge radius).

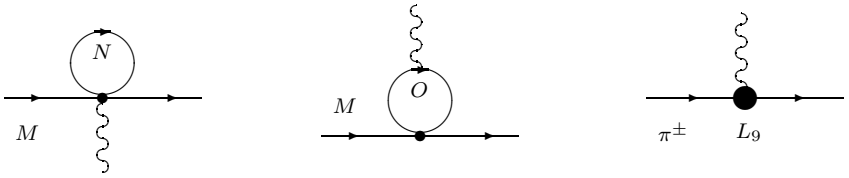

Figure 2: Strong insertions. a) Strong loops, where the photon is emitted at the vertex or through any charged meson O. M can be K_2^0, π^+, π^-. N denotes the allowed particles in the loop: π^0, π^+, K^+, η_8, K_1^0, K_2^0. b) Strong counterterm proportional to L_9 emitting a photon.

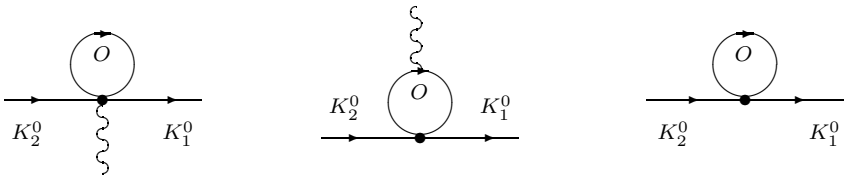

Figure 3: Strong loop insertions for the K_2^0 external line that mix the two CP eigenstates in the propagator. Their contribution, however, is finite.

The complete strong $\mathcal{O}(p^4)$ contribution to the amplitude is then obtained by summing up all diagrams where one replaced an external line in the diagrams of Figure 1 with a diagram from Figure 2 or Figure 3 in an appropriate way. It should be mentioned that, in principle, also wave function renormalization diagrams with counterterms proportional to L_4 and L_5 (Ref. [16]) (and suited loops) have to be considered. Due to the fact that the corresponding tree-level amplitude $K_2^0 \to \pi^+\pi^-\gamma^\star$ vanishes because of CP, however, these wave function renormalization diagrams do not contribute. One finds that the $K_2^0 - K_1^0$ propagator diagrams (from Figure 3) produce a finite contribution to the electric form factors, since there is no counterterm contribution to compensate a possible divergence. It is given by

$$\begin{aligned}\mathcal{F}_{11}^{Ll} &= \frac{-ieG_8}{(d-1)F}\frac{1}{[(p_1+p_2)^2-m_K^2]}(m_\pi^2+2p_1p_2)\cdot \\ &\quad \Big\{B(q^2,m_\pi^2,m_\pi^2)(4m_\pi^2-q^2)+(4-2d)A(m_\pi^2) \\ &\quad -B(q^2,m_K^2,m_K^2)(4m_K^2-q^2)-(4-2d)A(m_K^2)\Big\}. \qquad (20)\end{aligned}$$

The contributions of diagrams with insertions from Figure 2 also can be given in a very condensed and compact form:

$$\mathcal{F}_{12}^{Ll} = \frac{-ieG_8}{F}\cdot\Big\{-4q^2L_9 - \frac{d-2}{d-1}\Big[2A(m_\pi^2)+A(m_K^2)\Big] + \frac{1}{d-1}\cdot\Big[(4m_\pi^2-q^2)B(q^2,m_\pi^2,m_\pi^2)+\frac{1}{2}(4m_K^2-q^2)B(q^2,m_K^2,m_K^2)\Big]\Big\}. \quad (21)$$

The tadpole integral $A(m^2)$ and $B(p^2,m^2,m^2)$, the scalar two-propagator integral, are defined in Appendix A. Actually, the form factor F_{12}^{Ll} contains divergences stemming from the A and B functions which are renormalized by the strong counterterm coupling L_9 (coming from Figure 2b). Thus, in the finite amplitude with strong $\mathcal{O}(p^4)$ insertions, the measurable part of L_9 shows up: $L_9^r(770\ \text{MeV}) = (6.9\pm0.7)\cdot10^{-3}$. d is the spacetime dimension coming from dimensional regularization.

Weak counterterms only contribute through a diagram that is obtained from the direct emission diagram in Figure 1 by replacing the K_1^0 with the K_2^0 and the lowest-order vertex with the counterterm vertex. All occuring divergences from weak loop diagrams have to be removed by this single local counterterm contribution. The weak counterterms introduce the following contribution to the electric form factors:

$$\mathcal{F}_{13}^{Ll} = \frac{2ieG_8}{3F}q^2[N_{14}-N_{15}-3(N_{16}-N_{17})], \quad (22)$$

where all LECs except N_{17} depend on a scale which we choose to be 770 MeV. The coefficient Γ_{17} is found to vanish, which causes the independence of the renormalization scale. The renormalized parts of these couplings enter into the amplitude of the decay, therefore it is important to know their finite values.

The combination $(N_{14}^r - N_{15}^r)$ also appears in the counterterm amplitude of the decay $K^+\to\pi^+e^+e^-$ within the expression [23]

$$w_+ = \frac{64\pi^2}{3}[N_{14}^r(\mu)-N_{15}^r(\mu)+3L_9^r(\mu)] + \frac{1}{3}\ln(\frac{\mu^2}{m_K m_\pi}). \quad (23)$$

Old experiments [24] fixed w_+ to be $0.89^{+0.24}_{-0.14}$, which corresponds to a value of $(N_{14}^r - N_{15}^r) \simeq -0.02$ at the usual m_ρ scale. A more refined theoretical analysis of this decay took into account $\mathcal{O}(p^6)$ corrections to the form factor that describes the particular decay [25]. The polynomial part of this form factor is given by $W_+^{pol} = G_F m_K^2(a_+ + b_+ z)$, where $z = q^2/m_K^2$ and q is the momentum of the intermediate photon that gives rise to the lepton pair. The new parameter a_+ contains in principle also $\mathcal{O}(p^6)$ corrections and it is related with the usual w_+ through [25]

$$a_+ = \frac{G_8}{G_F}\Big[\frac{1}{3}-w_+\Big]. \quad (24)$$

A new experimental analysis of this decay [26] measured the parameters of the $K^+ \to \pi^+ e^+ e^-$ form factor and found $a_+ = -0.587 \pm 0.010$. With this new number we determine w_+ to be 1.086 and $(N_{14}^r - N_{15}^r) = -0.019 \pm 0.002$ and one finds that the two values are very much the same. (In Section 4.2, I determine the central value of $(N_{16}^r - N_{17})$ to be -0.014.)

The contributions of weak loops to the form factors are quite involved. To make everything more transparent how the different types of diagrams do contribute, I organize them in Figures 4 and 5 and quote their results separately. All weak tadpole diagrams can be obtained from the basic diagram (left) in Figure 4 by appending a photon on all charged lines and on the weak vertex. It turns out that only intermediate charged particles produce non-vanishing diagrams. The tadpole

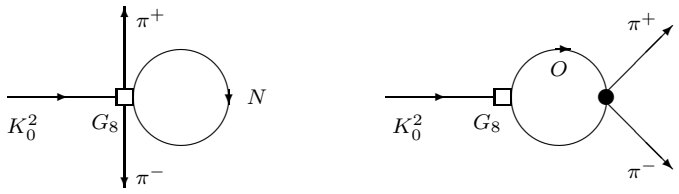

Figure 4: Weak loop diagrams: the basic tadpole diagram and the basic diagram of topology 1. N and O can be the same particles as in Figure 2.

part of the form factor looks very simple and reads as

$$\begin{aligned}\mathcal{F}_{14}^{Ll} &= \frac{-2ieG_8}{3F}\frac{1}{d-1}\Big\{2A(m_\pi^2)(2d-4) + 2B(q^2,m_\pi^2,m_\pi^2)(q^2-4m_\pi^2) \\ &\quad + A(m_K^2)(2d-4) + B(q^2,m_K^2,m_K^2)(q^2-4m_K^2)\Big\}. \qquad (25)\end{aligned}$$

Diagrams which can be constructed from the second diagram in Figure 4 are referred to as diagrams of topology 1. Again, one has to append a photon on all charged lines as well as on the strong and weak vertex. This time, only pairs of charged pions or charged kaons may occur in the loop. The contribution of topology 1 to the form factors is found to be very compact, too, and it is given by the following expression:

$$\begin{aligned}\mathcal{F}_{15}^{Ll} &= \frac{-ieG_8}{3F}\frac{1}{d-1}\Big\{2(2-d)A(m_\pi^2) - B(q^2,m_\pi^2,m_\pi^2)(q^2-4m_\pi^2) \\ &\quad + (2-d)A(m_K^2) - \frac{1}{2}B(q^2,m_K^2,m_K^2)(q^2-4m_K^2)\Big\}. \qquad (26)\end{aligned}$$

The diagrams considered so far produce form factors that are symmetric in the pion momenta p_1 and p_2. Besides, except A functions only $B(q^2, m^2, m^2)$ occurs and one can easily check that all these contributions vanish for an on-shell photon.

The decay amplitude is completed with the contributions from diagrams which belong to topologies 2 and 3. These diagrams are obtained from the basic diagrams in Figure 5 through the same steps as before. The expressions that one obtains from these graphs are rather involved, thus I will not present the results explicitly in terms of the standard scalar loop functions A, B, C that are defined in Appendix A. It is the contributions of these diagrams that introduce the asymmetry in p_1 and p_2 in the $\mathcal{O}(p^4)$ form factors. The possible pairs of particles in the loop are

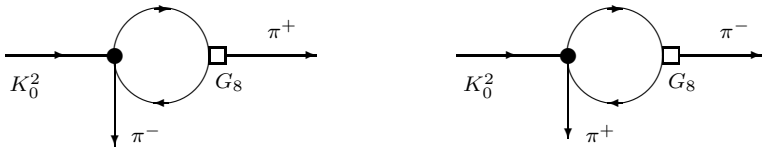

Figure 5: Weak loop diagrams: the basic diagram of topology 2 (left), the basic diagram of topology 3 (right).

(π^0, K^-), (η_8, K^-), (K_1^0, π^-), (K_2^0, π^-) for topology 2. The particles for topology 3 are the corresponding charge conjugated ones. It turns out that the diagrams with the internal combination (K_2^0, π^-) vanish. The contributions from the other three possible combinations to the form factor $\mathcal{F}_1^L$ are given in $\mathcal{F}_{16}^{Ll}$ in Appendix B, Eq. (47). By extracting only the explicit poles, one finds that all divergences are proportional to q^2, which corresponds to the counterterm parts of expressions (21) and (22). Furthermore, this shows that the corresponding decay with an on-shell photon is finite [20, 21]. Finally, the complete form factor $\mathcal{F}_1^L$ is given by

$$\mathcal{F}_1^L = \mathcal{F}_1^{Lt} + \mathcal{F}_{11}^{Ll} + \mathcal{F}_{12}^{Ll} + \mathcal{F}_{13}^{Ll} + \mathcal{F}_{14}^{Ll} + \mathcal{F}_{15}^{Ll} + \mathcal{F}_{16}^{Ll}. \tag{27}$$

As already mentioned above, the corresponding form factor $\mathcal{F}_2^L$ is obtained from $\mathcal{F}_1^L$ through the substitution $p_1 \leftrightarrow p_2$.

3.2 $K^+ \to \pi^+\pi^0\gamma^\star$ Amplitudes

Contrary to the K_L decay, there is no symmetry relation between the two electric form factors anymore, although the general structure of the amplitude stays the same as in (14). p_1 is now the momentum of the π^+ and p_2 the momentum of the π^0, respectively. Moreover, in the limit of isospin symmetry, the octet tree-level

amplitude vanishes. Hence, we relax the approximation of equal masses of charged and neutral pion at tree level and take the 27-plet coupling into account, too. In principle, the extraction of the 27-plet coupling G_{27} involves considerable uncertainties. Throughout the following analysis we will use $|G_8| = 9.1 \cdot 10^{-6}\text{GeV}^{-2}$ and $G_{27}/G_8 \simeq 1/18$, which is valid at tree level; of course, this simplification introduces an additional uncertainty in the prediction of the branching ratio. Nevertheless, the analysis in Ref. [17] suggests that G_{27} is only slightly modified by next-to-leading order corrections.

The tree-level form factors arise from the corresponding diagrams in Figure 1, where one has to replace the K_1^0 with the K^+ and the π^- with the π^0 and to remove a photon wherever it is necessary. Additionally, one has to exchange the coupling G_8 with the coupling G_{27}. Terms proportional to G_8 are clearly suppressed because of approximate isospin symmetry, thus the actual value of G_8 is not of much importance for the tree level. The lowest-order amplitude reads as

$$\begin{aligned}
\mathcal{F}_1^{+t} &= 2ieG_8F(m_{\pi^+}^2 - m_{\pi^0}^2)\Big\{\frac{1}{2qp_1+q^2} + \frac{1}{q^2-2qp}\Big\} \\
&\quad + \frac{2ieG_{27}F}{3}(5m_{K^+}^2 - 7m_{\pi^+}^2 + 2m_{\pi^0}^2)\frac{2qp_2}{(q^2+2qp_1)(q^2-2qp)}, \\
\mathcal{F}_2^{+t} &= \frac{2ieF}{q^2-2qp}\Big[G_8(m_{\pi^+}^2 - m_{\pi^0}^2) - \frac{2G_{27}}{3}(5m_{K^+}^2 - 7m_{\pi^+}^2 + 2m_{\pi^0}^2)\Big].
\end{aligned} \tag{28}$$

The magnetic form factor at lowest order ($\mathcal{O}(p^4)$) is derived from the counterterm Lagrangian (12) and the WZW Lagrangian (13) and it is therefore necessarily finite. One finds the following expression:

$$\mathcal{M}^+ = \frac{eG_8}{4\pi^2 F}(2 - 3a_2 + 6a_3), \tag{29}$$

where the 2 comes from the Lagrangian (13). Again, the values for these couplings are not known. But the magnetic form factor $\mathcal{M}^+$ turns out to be the same as in the case of the corresponding radiative K^+ decay [21], which suggests to use results from the E787 experiment [14] to estimate the combination of LECs in (29). The authors report a branching ratio from direct emission of $\text{BR}(K^+ \to \pi^+\pi^0\gamma; \text{DE}, 55\ \text{MeV} < T_{\pi^+} < 90\ \text{MeV}) = (4.7 \pm 0.8(\text{stat.}) \pm 0.3(\text{syst.})) \cdot 10^{-6}$. Under the rather reasonable assumption that direct emission is entirely due to the magnetic amplitude, one can extract a value for the whole combination above. Of course, this does not take into account energy dependent corrections, but this is at the moment the best one can do. Moreover, the experimental data seem to indicate that neglect of these higher-order terms does not do much harm to the magnetic amplitude. The authors also find no evidence for any electric direct emission in the

decay [14]. Using $\mathcal{A}(K^+ \to \pi^+\pi^0\gamma, DE) = \mathcal{M}^+\epsilon^{\mu\nu\rho\sigma}p_{1\nu}p_{2\rho}q_\sigma\epsilon^\star_\mu(q)$, one can extract for the combination in question from the radiative decay ($q^2 = 0$)

$$|A_4| = |2 - 3a_2 + 6a_3| = 2.26 \pm 0.25. \tag{30}$$

Again, I start to discuss the contributions of strong loops and strong counterterm diagrams to the electric form factors. From now on, strong isospin is conserved and 27-plet corrections are neglected.

Diagrams with strong loops and strong counterterm vertices arise only through insertions of these loops and vertices in propagators or external lines in diagrams corresponding to those in Figure 1. The relevant tree-level diagrams are obtained from Figure 1 by replacing $K_1^0 \to K^+$ and $\pi^- \to \pi^0$. The needed insertions are obtained from the diagrams in Figure 2 , where M can be K^+, π^+, π^0 and N is one of π^+,π^0, K^+, K^0, $\bar{K}^0$, η_8, respectively. Thus, the final strong contribution to the next-to-leading order part of the form factors reads as:

$$\begin{aligned}\mathcal{F}_{11}^{+l} &= \frac{-ieG_8}{F}\cdot\Big\{-4q^2L_9 - \frac{d-2}{d-1}\Big[2A(m_\pi^2) + A(m_K^2)\Big] + \frac{1}{d-1}\cdot \\ &\quad \Big[(4m_\pi^2 - q^2)B(q^2, m_\pi^2, m_\pi^2) + \frac{1}{2}(4m_K^2 - q^2)B(q^2, m_K^2, m_K^2)\Big]\Big\},\end{aligned} \tag{31}$$

whereas $\mathcal{F}_{21}^{+l} = 0$, which is due to the fact that the π^0 is neutral. Again, wave function renormalization diagrams do not contribute to the final amplitude because the tree-level octet amplitude for $K^+ \to \pi^+\pi^0\gamma^\star$ vanishes in the isospin limit. The coupling L_9 renormalizes the sum of these diagrams that vanishes in the case of an on-shell photon.

Substituting the relevant weak counterterm vertex for the lowest-order vertex in the direct emission diagram in Figure 1 and making the necessary particle replacements, one calculates this local contribution to the form factors:

$$\begin{aligned}\mathcal{F}_{12}^{+l} &= \frac{-ieG_8}{3F}\Big[-6qp_2(N_{14} - N_{15} - N_{16} - N_{17}) - 4q^2(N_{14} - N_{15})\Big], \\ \mathcal{F}_{22}^{+l} &= \frac{-ieG_8}{3F}\Big[6qp_1(N_{14} - N_{15} - N_{16} - N_{17}) - 2q^2(N_{14} + 2N_{15}) \\ &\qquad +6q^2(N_{16} - N_{17})\Big].\end{aligned} \tag{32}$$

One recovers the finite combination $(N_{14} - N_{15} - N_{16} - N_{17})$ of the on-shell decay and the related structure which is governed by gauge invariance [20, 21]. Making use of the now determined combination $(N_{16}^r - N_{17})$ and appealing to some theoretical models for weak counterterms, (32) and therefore the whole amplitude finally contain only one unknown combination, $(N_{14}^r + 2N_{15}^r)$. I will come back to this later. The divergences that arise from weak loop diagrams which I will consider next are

renormalized by these combinations.

Weak tadpole diagrams can be constructed from the basic diagram in Figure 4 (with $K_2^0 \to K^+$, $\pi^- \to \pi^0$) through the corresponding steps as in 3.1 and one obtains

$$\begin{aligned}
\mathcal{F}_{13}^{+l} &= \frac{-ieG_8}{3F}\frac{1}{d-1}\Big\{(2d-4)A(m_\pi^2) + B(q^2,m_\pi^2,m_\pi^2)(q^2-4m_\pi^2) \\
&\quad +(2d-4)A(m_K^2) + B(q^2,m_K^2,m_K^2)(q^2-4m_K^2)\Big\}, \\
\mathcal{F}_{23}^{+l} &= \frac{-ieG_8}{3F}\frac{1}{d-1}\Big\{(2d-4)A(m_\pi^2) + B(q^2,m_\pi^2,m_\pi^2)(q^2-4m_\pi^2) \\
&\quad -(2d-4)A(m_K^2) - B(q^2,m_K^2,m_K^2)(q^2-4m_K^2)\Big\}. \qquad (33)
\end{aligned}$$

One finds that η_8 loops do not contribute. In the case of an on-shell photon, expressions (33) vanish.

Diagrams of the topology 1 are constructed from the second diagram in Figure 4 (with the same replacements as already mentioned), where one has to replace the charged meson pairs in the loops with (π^+,π^0), $(K^+,\bar{K}^0)$, or with (π^+,η_8) (in an appropriate momentum convention). The last combination of intermediate particles vanishes in the isospin limit. Appending a photon where it is possible and summing up the diagrams, one finds that the result is very compact and that it involves only A and $B(q^2,m^2,m^2)$ functions:

$$\begin{aligned}
\mathcal{F}_{14}^{+l} &= \frac{-ieG_8}{F(d-1)}\Big\{(d-2)\Big[A(m_K^2)+\frac{4}{3}A(m_\pi^2)\Big] \\
&\quad +\frac{1}{2}B(q^2,m_K^2,m_K^2)(q^2-4m_K^2) + \frac{2}{3}B(q^2,m_\pi^2,m_\pi^2)(q^2-4m_\pi^2)\Big\}, \\
\mathcal{F}_{24}^{+l} &= \frac{-ieG_8}{F(d-1)}\Big\{(2-d)\Big[A(m_K^2)+\frac{2}{3}A(m_\pi^2)\Big] \\
&\quad +\frac{1}{2}B(q^2,m_K^2,m_K^2)(4m_K^2-q^2) + \frac{1}{3}B(q^2,m_\pi^2,m_\pi^2)(4m_\pi^2-q^2)\Big\}. \qquad (34)
\end{aligned}$$

Expressions (34) vanish in the on-shell limit and their divergences are clearly proportional to q^2. The last and by far most voluminous contribution to the electric $\mathcal{O}(p^4)$ form factors comes from diagrams of the topologies 2 and 3 which can be derived from the basic diagrams in Figure 5 as before. Possible virtual pairs are (K^-,π^0), (K^+,η_8), (K^0,π^-) and (K^0,π^0), (K^0,η_8), (K^+,π^-), respectively. These form factors, $\mathcal{F}_{15,16}^{+l}$ and $\mathcal{F}_{25,26}^{+l}$, are listed in Appendix C, (48), (49) and (50), (51). Finally, the complete form factor $\mathcal{F}_1^+$ is given by

$$\mathcal{F}_1^+ = \mathcal{F}_1^{+t} + \mathcal{F}_{11}^{+l} + \mathcal{F}_{12}^{+l} + \mathcal{F}_{13}^{+l} + \mathcal{F}_{14}^{+l} + \mathcal{F}_{15}^{+l} + \mathcal{F}_{16}^{+l}; \qquad (35)$$

$\mathcal{F}_2^+$ is obtained from the corresponding equation.

4 Numerical analysis

4.1 Decay width

The decay width for the processes in question is given by the following standard formula:

$$\Gamma(K \to \pi_1\pi_2 e^+e^-) \;=\; \frac{m_e^2}{128\pi^8 m_K}\int \frac{d^3p_1}{2E_1}\frac{d^3p_2}{2E_2}\frac{d^3k_+}{2E_+}\frac{d^3k_-}{2E_-}\delta^{(4)}(p_f-p_i)\sum_{spins}|\mathcal{A}|^2, \tag{36}$$

where p_1 is always the momentum of the positive pion and p_2 refers to the corresponding other pion, π^- or π^0. As usual, $p_{i,f}$ are the sums of ingoing momenta and of outgoing momenta. In fact, $p_i^\mu = (m_K, 0, 0, 0)$. The squared transition amplitude for both decays in question reads as (with the convention $\epsilon^{0123} = 1$)

$$\begin{aligned}
\sum_{spins}|\mathcal{A}|^2 \;=\; & \frac{e^2}{m_e^2q^4}\Big\{-(m_e^2+k_+k_-)\Big[|\mathcal{F}_1|^2p_1^2+|\mathcal{F}_2|^2p_2^2+p_1p_2(\mathcal{F}_1\mathcal{F}_2^\star+\mathcal{F}_1^\star\mathcal{F}_2)\Big] \\
& +2|\mathcal{F}_1|^2k_+p_1k_-p_1+2|\mathcal{F}_2|^2k_+p_2k_-p_2+(\mathcal{F}_1\mathcal{F}_2^\star+\mathcal{F}_1^\star\mathcal{F}_2) \\
& (k_+p_1k_-p_2+k_-p_1k_+p_2)\Big\}+\frac{e^2|\mathcal{M}|^2}{m_e^2q^4}\Big\{(-m_e^2+k_+k_-)\Big[p_1^2qp_2^2 \\
& +p_2^2qp_1^2+q^2p_1p_2^2-p_1^2p_2^2q^2-2p_1p_2qp_1qp_2\Big]+2qk_-qk_+ \\
& (p_1^2p_2^2-p_1p_2^2)+2k_-p_1k_+p_1(p_2^2q^2-qp_2^2)+2k_-p_1k_+p_2(p_1^2q^2-qp_1^2) \\
& +2(qp_1qp_2-q^2p_1p_2)(k_+p_1k_-p_2+k_+p_2k_-p_1)+2(p_1p_2qp_2-p_2^2qp_1) \\
& (k_+p_1k_-q+k_-p_1k_+q)+2(p_1p_2qp_1-p_1^2qp_2)(k_+p_2k_-q+k_-p_2k_+q)\Big\} \\
& +\frac{e^2}{m_e^2q^4}\epsilon^{\mu\nu\rho\sigma}k_{-\mu}p_{1\nu}p_{2\rho}k_{+\sigma}\Big\{(k_+p_1-k_-p_1)(\mathcal{F}_1^\star\mathcal{M}+\mathcal{F}_1\mathcal{M}^\star) \\
& +(k_+p_2-k_-p_2)(\mathcal{F}_2^\star\mathcal{M}+\mathcal{F}_2\mathcal{M}^\star)\Big\}.
\end{aligned} \tag{37}$$

The structure of (37) implies that there is no interference between electric and magnetic form factors in the decay widths of these decays. Additionally, one finds in the case of K_L that there is no interference between electric form factors of lowest and next-to-leading order, too. This feature is due to their different behaviour under exchange of pion momenta. Branching ratios thus consist of three distinct contributions. The more general case of interference between different electric parts is present in the K^+ decay. Phase space integrations are performed numerically with the Fortran event generator RAMBO [27].

4.2 Numerical analysis of $K_L \to \pi^+\pi^-e^+e^-$

In general, the branching ratios are given for different cuts in q^2, i.e., for different lower bounds on $(k_+ + k_-)^2$. Throughout this analysis, I use the central values of experimental numbers for the branching ratios with certain cuts in q^2. Additionally, I quote the error of the predicted branching ratio if it is calculated over the whole phase space. It should be pointed out (compared to Ref. [4]) that the KTeV data , on which I will rely in the following analysis, are corrected for the entire phase space [9, 10, 13].

$q^2 >$ [MeV^2]	Magnetic BR [10^{-8}]	Tree-level BR [10^{-8}]
2^2	18.20	9.8
10^2	9.31	2.95
20^2	5.61	1.33
30^2	3.65	0.71
40^2	2.42	0.41
60^2	1.06	0.16
80^2	0.44	0.061
100^2	0.16	0.024
120^2	0.053	0.009
180^2	0.00025	0.0001
entire p.s.	21.2 ± 9.0	12.8 ± 1.0

Table 1: Magnetic and tree-level contributions to the branching ratio of $K_L \to \pi^+\pi^-e^+e^-$ for different cuts in q^2 and for the entire phase space.

Using ansatz (19) and the experimental numbers of [9] as input for the magnetic contribution to the branching ratio, I find the results that are collected in Table 1. Neglecting the energy dependent part in (19) one reproduces the numbers of Ref. [3]. Consideration of the energy dependent magnetic form factor in (19) increases the result, particularly for low cuts. Table 1 also shows the importance of the q^2 range between $4m_e^2$ and 4 MeV^2 which was not considered in Ref. [4]. The reason for this can be understood from the plot of the differential decay widths of the individual contributions to the decay in Figure 6. Unfortunately, the errors of the parameters that enter into the magnetic contribution are rather large [9], thus the magnetic branching ratio over the whole phase space has a considerable uncertainty.

The tree-level form factors of (17) give rise to the results collected in column three of Table 1. Comparison with the results in Ref. [3] shows that the obtained numbers are rather different, but this is due to different values of F and G_8. Here, we use $F = 92.4$ MeV and $G_8 = 9.1 \cdot 10^{-6}\text{GeV}^{-2}$. The error of the BR over the entire

phase space in the last line comes from numerics and reflects the $1/q^4$ behaviour of the squared amplitude. Applying the bremsstrahlung approximation one finds that the results in the third column are increased; for a lower cut of $(20\ \mathrm{MeV})^2$ by about 4%, for a cut of $(60\ \mathrm{MeV})^2$ by about 18%. On the other hand, it is clear that these deviations from the results in Table 1 do not at all affect the BR and that the use of the larger G_8 is justified.

The $\mathcal{O}(p^4)$ electric form factors depend via (22) quadratically on $(N_{16}^r - N_{17}) =: x$ which is counted in units of 10^{-2}. Their contributions to the branching ratio are listed in Table 2. The error was estimated by taking into account the uncertainties of L_9^r and $(N_{14}^r - N_{15}^r)$. The numbers cannot be compared directly to the results in Ref.

$q^2 > [\mathrm{MeV}^2]$	Loops+Counterterms BR $[10^{-8}]$
2^2	$0.22 - 0.68x + 0.54x^2$
10^2	$0.22 - 0.67x + 0.53x^2$
20^2	$0.21 - 0.66x + 0.52x^2$
30^2	$0.20 - 0.63x + 0.49x^2$
40^2	$0.19 - 0.59x + 0.46x^2$
60^2	$0.16 - 0.48x + 0.37x^2$
80^2	$0.12 - 0.36x + 0.27x^2$
100^2	$0.08 - 0.24x + 0.18x^2$
120^2	$0.05 - 0.14x + 0.10x^2$
180^2	$0.002 - 0.005x + 0.004x^2$
entire p.s.	$0.22 \pm 0.11 - (0.68 \pm 0.16)x + 0.54x^2$

Table 2: Contributions of loop diagrams and electric counterterms for different cuts in q^2 and for the entire phase space to the branching ratio of $K_L \to \pi^+\pi^- e^+ e^-$ as functions of the unknown combination of counterterms $(N_{16}^r - N_{17}) =: x\ [10^{-2}]$.

[3], since these authors express the corresponding branching ratios as functions of a different combination of LECs, w_L [3]. It turns out that this w_L is connected with the used N_i through $8\pi^2(-N_{14}^r + N_{15}^r + N_{16}^r - N_{17})$. Moreover, a different renormalization scale and a modified renormalization scheme were used. It is obvious from Table 2 that the electric $\mathcal{O}(p^4)$ contributions are nearly insensitive to changes of the cut below $(60\ \mathrm{MeV})^2$. This feature becomes clear from inspection of Figure 6.

Theory finally predicts $(21.2 + 12.8 + 0.22 - 0.68x + 0.54x^2) \cdot 10^{-8}$, with $x = (N_{16}^r - N_{17})[10^{-2}]$ as central value for the BR over the entire phase space. Comparison with Ref. [1], BR = [18 (magn.)+13 (tree)+0.4 (CR)]$\cdot 10^{-8}$, shows that inclusion of the magnetic form factor of Ref. [9] increases the magnetic BR considerably. Also the total $\mathcal{O}(p^4)$ electric contribution of Table 2 changes the result to some extent.

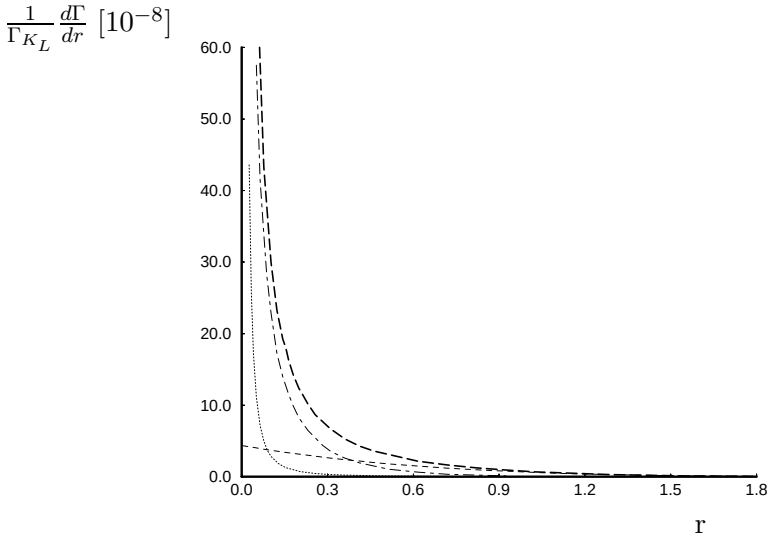

Figure 6: Differential decay width $\frac{1}{\Gamma_{K_L}}\frac{d\Gamma}{dr}$ for $(N_{16}^r - N_{17}) = -0.014$; $r := q^2/m_\pi^2$ and $\frac{d\Gamma}{dq^2} = \frac{1}{m_\pi^2}\frac{d\Gamma}{dr}$. The dotted line is the tree-level contribution, the dashed line is loops and counterterms, the dot-dashed line is the magnetic part. The thick long-dashed line is the sum. Γ_{K_L} is the total width of the K_L. For cuts with $q^2 > (130\text{ MeV})^2$ the differential decay width is dominated by the contributions of the electric $\mathcal{O}(p^4)$ amplitude, i.e., loops and electric counterterms.

In the following, the obtained theoretical BR will be compared to the most recent available data. Contrary to Ref. [3] and Ref. [4], where a cut of $q^2 = (2\text{ MeV})^2$ was applied, the energy dependence of the magnetic form factor is taken into account as well as the BR over the entire phase space. I focus on the data of the KTeV collaboration, but for completeness one should mention that the NA48 experiment at CERN reported a preliminary BR of $(2.90\pm0.15)\cdot10^{-7}$ [13], based on 458 events, and that a Japanese group obtained a BR of $(4.4\pm1.3(\text{stat.})\pm0.5(\text{syst.}))\cdot10^{-7}$ [7] which is based on 13 events. In the last two years, the KTeV result of the corresponding branching ratio was subject to numerous analyses and the errors improved quite a lot. The first published BR was based on a sample of 46 events and was found to be $(3.2 \pm 0.6(\text{stat.}) \pm 0.4(\text{syst.})) \cdot 10^{-7}$ [5]. A new analysis based on the full 1997 data set reported a BR of $(3.32\pm0.14(\text{stat.})\pm0.28(\text{syst.}))\cdot10^{-7}$ with a much better statistical error [10]. I am going to use the latest available (preliminary) numbers which are again obtained from the 1997 data set by considering the parametrization

Model	Prediction	$(N_{14}^r - N_{15}^r) - x_1$	$(N_{14}^r - N_{15}^r) - x_2$
WDM	-0.004	-0.046 ± 0.036	-0.005 ± 0.036
FM	$-0.007 k_f$		

Table 3: Comparison of model predictions (WDM, FM) and the two possible values extracted from data for the combination $(N_{14}^r - N_{15}^r) - (N_{16}^r - N_{17})$.

in (19) [13]: BR $= (3.63 \pm 0.11(\text{stat.}) \pm 0.14(\text{syst.})) \cdot 10^{-7}$. According to Ref. [13], the difference in the KTeV and CERN results is due to the usage of the magnetic form factor.

It is clear that it is not possible to determine unambiguously the value of x only by comparison with the experiment. The two possible values of x are

$$\begin{aligned} (N_{16}^r - N_{17})_1 &= x_1 = (2.7 \pm 3.6) \cdot 10^{-2}, \\ (N_{16}^r - N_{17})_2 &= x_2 = (-1.4 \pm 3.6) \cdot 10^{-2}. \end{aligned} \tag{38}$$

The large error is mostly ($\sim$ 80%) due to the uncertainty of the magnetic BR. There is even a small overlap of the two ranges. Moreover, it should be stressed that comparison with the BR over the entire phase space is not the best possibility to extract values for the LECs, since then the BR is dominated by the tree level and the magnetic amplitude. Figure 6 suggests that one could extract these values more precisely for much higher cuts in q^2, but this is not possible at the moment. Nevertheless, the central values are very different and one can appeal to some models of weak counterterm couplings to distinguish between the two solutions. The Weak Deformation Model (WDM) and the Factorization Model (FM) [19] make predictions about the involved LECs, but besides a free parameter (FM), N_{14}^r and N_{16}^r depend additionally (in both models) on the contact term coupling L_{11} from the strong counterterm Lagrangian [16], which makes it necessary to compare $(N_{14}^r - N_{15}^r) - (N_{16}^r - N_{17})$ with the experimental values. The comparison of prediction and experiment is given in Table 3. k_f parametrizes the factorization hypothesis and is expected to be of $\mathcal{O}(1)$. Comparison with the results in Table 3 gives $k_{f1} \simeq 6.4 \pm 5.0$ and $k_{f2} \simeq 0.7 \pm 5.0$, respectively. First of all, it is remarkable to find the central value of x_2 to be in such good agreement with the predictions of the two models. Second, the errors are big enough to dampen too much enthusiasm, but anyway, the solution $(N_{16}^r - N_{17}) = -0.014$ is clearly favoured by both models. Moreover, both models and the calculations of Bruno and Prades [28] suggest that N_{17} vanishes individually, so one can even go one step further and assume that

$$N_{16}^r = (-1.4 \pm 3.6) \cdot 10^{-2} \ , \quad N_{17} = 0. \tag{39}$$

Additional supporting experimental input comes from the null measurement of an interference between electric and magnetic parts of the $K^+ \to \pi^+\pi^0\gamma$ amplitude in Ref. [14], since this indicates that the combination $(N_{14}^r - N_{15}^r - N_{16}^r - N_{17}) \simeq 0$ or very small [20, 21]. Assumption (39), however, is only true for a certain class of models and one should take into account other models, too, e.g., the modified FM (FMV) [29] by D'Ambrosio and Portolés, who do predict in general a N_{17} different from 0. In any case, solution x_2 is also preferred by the approach in Ref. [29]. We will consider the FMV approach more closely in the next chapter.

If one's trust in the models used above were big enough, one could even use (39) to calculate the contact term coupling L_{11} of Ref. [16] and, as a consequence, calculate N_{14}^r and N_{15}^r individually, but this does not seem to make much sense. Anyway, assumption (39) serves as a solid starting point for the analysis of the K^+ decay.

4.3 Numerical analysis of $K^+ \to \pi^+\pi^0 e^+ e^-$

As in the previous case, there is again no interference between magnetic and electric parts of the amplitude. Because of the absence of a symmetry relation like in the K_L decay between the electric form factors, this time there is interference between the tree-level amplitude and the loops and electric counterterm parts.

For the purely magnetic part of the branching ratio, the value of (30) is used. The results are collected in the second column of Table 4. As in Section 4.2, I only quote the error associated with A_4 for the branching ratio over the entire phase space.

In the following, I present the individual electric as well as the total electric branching ratios, which allows for an extraction of the interference contribution. This interference part is given by a linear function in the remaining unknown combination of LECs. The BR due to the lowest order is generated by the tree-level form factors given in (28). They produce a branching ratio that is much larger than in the case of $K_L \to \pi^+\pi^- e^+ e^-$; it is given in the third column of Table 4. As already mentioned above, the tree-level value of G_{27} is used for the numerical analysis and this clearly introduces an intrinsic uncertainty in the predictions. Therefore, for completeness, I only quote the error that arises from numerics because of the $1/q^4$ behaviour of the tree-level amplitude. In any case, this error is much smaller than the one associated with the error of $(N_{16}^r - N_{17})$. The error associated with the choice of G_8 is very small in case of the tree level. For the case of loop and counterterm contributions, this error is of next-to-next-to-leading order.

The $\mathcal{O}(p^4)$ form factors contain the combinations of LECs given in (32). Here, I use the assumption of (39) and thus can express the results in terms of $(N_{14}^r + 2N_{15}^r) =: z$ (in units of 10^{-2}) (Table 5a). The total electric contributions are col-

$q^2 >$ [MeV^2]	Magnetic BR [10^{-8}]	Tree-level BR [10^{-8}]
2^2	5.33	254.20
10^2	2.84	74.33
20^2	1.80	32.51
30^2	1.23	17.35
40^2	0.86	10.04
60^2	0.42	3.75
80^2	0.19	1.46
100^2	0.083	0.56
120^2	0.031	0.20
180^2	0.0002	0.002
entire p.s.	6.14 ± 1.29	330 ± 15

Table 4: Magnetic and tree-level contributions to the branching ratio of $K^+ \to \pi^+\pi^0 e^+ e^-$ for different cuts in q^2 and for the entire phase space. The error of the magnetic part is due to experimental uncertainties of $|A_4|$, while the error from the tree-level part comes from numerics; additionally, there is an intrinsic uncertainty because of the G_{27} coupling.

lected in Table 5*b*. From this analysis it is clear that the $\mathcal{O}(p^4)$ corrections to the branching ratio will be very difficult to distinguish by experiment. Again, the importance of the last step from a cut of 4 MeV^2 to no cut at all should be mentioned. Comparison with the previous K_L decay shows that the tree-level contribution dominates the BR, although it is suppressed by isospin symmetry, and that it is much more important than in the K_L case, where the tree level was suppressed because of CP.

Finally, using only the central values of input quantities and applying assumption (39), $N_{16}^r = -0.014$ and $N_{17} = 0$, the BR for $K^+ \to \pi^+\pi^0 e^+ e^-$ over the entire phase space is predicted to be $[6.14 \ + \ 378 + 0.27z + 0.004z^2] \cdot 10^{-8}$.

4.4 Dependence on counterterm models

In Section 4.2 it was claimed that also the FMV of Ref. [29] favours $(N_{16}^r - N_{17}) = -0.014$. We will now clarify why this is so. In Ref. [29], the authors follow a different approach to the evaluation of weak LECs in terms of vector and axial-vector resonance exchange contributions compared to Ref. [19]. In their framework (FMV), combinations of LECs are functions of two positive $\mathcal{O}(1)$ parameters, η_V and η_A. In the FMV, the combination $(N_{14}^r - N_{15}^r) = -0.020\eta_V + 0.004\eta_A$ and

$q^2 >$ [MeV^2]	BR $[10^{-9}]$	BR $[10^{-9}]$
	Loops+Counterterms	Electric $\mathcal{O}(p^2) + \mathcal{O}(p^4)$
2^2	$46.50 + 0.51z + 0.042z^2$	$2745 + 2.69z + 0.042z^2$
10^2	$2.52 + 0.48z + 0.042z^2$	$785.6 + 2.57z + 0.042z^2$
20^2	$1.68 + 0.46z + 0.041z^2$	$354.3 + 2.29z + 0.041z^2$
30^2	$1.43 + 0.43z + 0.039z^2$	$193.8 + 2.09z + 0.039z^2$
40^2	$1.25 + 0.40z + 0.036z^2$	$115.6 + 1.83z + 0.036z^2$
60^2	$0.94 + 0.32z + 0.030z^2$	$46.3 + 1.32z + 0.030z^2$
80^2	$0.67 + 0.24z + 0.022z^2$	$19.8 + 0.88z + 0.022z^2$
100^2	$0.43 + 0.16z + 0.015z^2$	$8.40 + 0.52z + 0.015z^2$
120^2	$0.25 + 0.09z + 0.009z^2$	$3.34 + 0.27z + 0.009z^2$
180^2	$0.01 + 0.004z + 0.0004z^2$	$0.06 + 0.008z + 0.0004z^2$
entire p.s.	Loops+Countert.	$122 \pm 134 + (0.56 \pm 0.27)z + 0.043z^2$
entire p.s.	El. $\mathcal{O}(p^2) + \mathcal{O}(p^4)$	$3783 \pm 350 + (2.74 \pm 0.82)z + 0.043z^2$

Table 5: a) Pure electric $\mathcal{O}(p^4)$ contribution to the branching ratio for different cuts in q^2. b) Contributions to the branching ratio for different cuts in q^2 from the total electric part, $\mathcal{O}(p^2)$ and $\mathcal{O}(p^4)$. c) Branching ratios for the entire phase space with consideration of the error of (39). $(N_{14}^r + 2N_{15}^r) := z\ [10^{-2}]$.

$(N_{14}^r - N_{15}^r) - 3(N_{16}^r - N_{17}) = -0.004\eta_V + 0.018\eta_A$, respectively. Comparison with the two possible values of $(N_{16}^r - N_{17})$ in (38) gives the following results for the parameters: for $(N_{16}^r - N_{17}) = 0.027$, one finds

$$\eta_{V_1} = -0.2 \pm 1.1 \quad \text{and} \quad \eta_{A_1} = -5.6 \pm 5.8. \tag{40}$$

Using $(N_{16}^r - N_{17}) = -0.014$, one calculates for the FMV parameters

$$\eta_{V_2} = 1.3 \pm 1.1 \quad \text{and} \quad \eta_{A_2} = 1.6 \pm 5.8. \tag{41}$$

Of course, the errors are very big, but even then the second set of parameters in (41) fits much better than those of (40). Using the parametrization of the combination $(N_{14}^r - N_{15}^r) - 3(N_{16}^r + N_{17}) = 0.05\eta_V - 0.04\eta_A$, one determines $N_{17} = -0.009\eta_V + 0.0097\eta_A = 0.4 \cdot 10^{-2}$. Thus, we rather find for N_{16}^r and N_{17} with the parameters of (41)

$$\begin{aligned} N_{16}^r &= (-1.0 \pm 4.6) \cdot 10^{-2}, \\ N_{17} &= (0.4 \pm 4.6) \cdot 10^{-2} \end{aligned} \tag{42}$$

In fact, this result is not too different from the hypothesis in (39).

$q^2 >$ [MeV^2]	electric BR with (42), (43) [10^{-9}]
2^2	2923
10^2	873
20^2	431
30^2	253
40^2	164
60^2	78
80^2	39
100^2	20
120^2	9
180^2	0.24
entire p.s.	3683

Table 6: The total electric BR for different cuts and for the entire phase space relying on the FMV and using the parameter values calculated in (42) and (43). No errors are taken into account.

Despite the big uncertainties of the η_V and η_A parameters, one nevertheless can use their central values to calculate other LECs, especially N_{14}^r and N_{15}^r. Probably this is equally daring as the option of calculating L_{11}, but if one truly 'believed' in the FMV with the parameters of (41), one could make a parameter-free prediction for the electric part of the branching ratio. According to Ref. [29], we can express $2N_{14}^r + N_{15}^r = 0.08\eta_V$. Using the experimental result $(N_{14}^r - N_{15}^r) = -0.019$, one calculates:

$$\begin{aligned} N_{14}^r &= 2.8 \cdot 10^{-2}, \\ N_{15}^r &= 4.7 \cdot 10^{-2}. \end{aligned} \tag{43}$$

The results for the branching ratios obtained with these values for the counterterm couplings are listed in Table 6. According to Table 5, one finds that $\mathcal{O}(p^4)$ corrections become more important for higher cuts in q^2 and that branching ratios for lower cuts are dominated by the tree level. E.g., for a cut of (10 MeV)^2, the BR is modified by pure $\mathcal{O}(p^4)$ corrections and by the interference between the two electric contributions by about 17%, whereas for a cut of (80 MeV)^2 the result is increased by about 160%. It is clear that the interference also gives rise to an important part of the enhancement of the BR. Finally, one should note that the estimated couplings in (42) and (43) are in a range where one would expect them but, of course, also that the uncertainties involved are too big to make a more precise statement about the couplings and the K^+ decay width.

5 Conclusions

I considered the non-leptonic decays $K_L \to \pi^+\pi^- e^+ e^-$ and $K^+ \to \pi^+\pi^0 e^+ e^-$ within the framework of Chiral Perturbation Theory. First of all, the amplitudes of the decays have been given up to order p^4 in a very explicit way. A consistency check on parts of the weak counterterm Lagrangian of CHPT was performed: all divergences are properly removed.

The main interest in the decay $K_L \to \pi^+\pi^- e^+ e^-$ in this paper is not CP-violation as in Ref. [3] but the possibility of the extraction of $(N_{16}^r - N_{17})$ from experimental results. The latest values of the BR (preliminary $(3.63 \pm 0.11 \pm 0.14) \cdot 10^{-7}$) and of the two parameters of a magnetic form factor that were obtained by the KTeV collaboration were used for the numerical analysis of the decay. The introduction of an energy dependent magnetic form factor is an important correction to the older calculations in Ref. [3], since it increases the magnetic contribution to the branching ratio considerably. The (preliminary) value for the branching ratio as well as the parameters of the magnetic form factor were obtained from the analysis of the data set of 1997 which contains more than 1800 events. Comparison with earlier results shows that the errors of the measured quantities became quite smaller due to the better statistics but the uncertainties are still too big to make precise predictions.

Comparison with experiment yields two possible values of the LEC combination $(N_{16}^r - N_{17})$, thus one has to take into account theoretical models of weak counterterm couplings to distinguish between the possible solutions. All models that have been considered (Weak Deformation Model WDM, Factorization Model FM, Modified Factorization Model FMV) prefer the same value of $(-1.4 \pm 3.6) \cdot 10^{-2}$. Of course, the error is quite large, which is mainly due to the experimental uncertainties of the two parameters of the magnetic amplitude, but nevertheless, the chosen result is reasonable compared with $(N_{14}^r - N_{15}^r) = -1.9 \cdot 10^{-2}$ and it rests on a firm theoretical ground. Since 1997, much more data have been collected by the KTeV group and therefore one can hope that a new analysis of the much bigger set of events can reduce the experimental uncertainties. As already mentioned above, it should also be possible to extract the value of $(N_{16}^r - N_{17})$ to a better precision by comparing the theoretical results with branching ratios for higher cuts in q^2, since the contributions from loops and counterterms become much more important for higher cuts than for the entire phase space. The central value of $(N_{16}^r - N_{17})$, however, is in nearly perfect agreement with the FM and WDM predictions. One also derives central values for the parameters of the FMV that are in good agreement with the expectations.

To be able to make a useful prediction for the K^+ decay, one has to rely on additional theoretical assumptions. First, I followed the predictions of the FM and WDM and assumed that the extracted value $(-1.4) \cdot 10^{-2}$ is produced solely by N_{16}^r and that $N_{17} = 0$. The branching ratio for $K^+ \to \pi^+\pi^0 e^+ e^-$ therefore is finally

expressed as a function of $(N_{14}^r + 2N_{15}^r)$ only. Contrary to the K_L decay above, there is an interference between the tree-level amplitude and the electric $\mathcal{O}(p^4)$ amplitude. It is found that, in general, the branching ratio is dominated by the electric part of the decay amplitude. Moreover, it is the tree level that produces by far the most important contributions, for the entire phase space as well as for cuts in q^2. An extraction of the combination $(N_{14}^r + 2N_{15}^r)$ from the BR over the entire phase space is almost impossible, but with a scan of the q^2 spectrum it could be possible to extract values for $(N_{14}^r + 2N_{15}^r)$, especially for cuts larger than $(60\ \mathrm{MeV})^2$. It is obvious that the experimental error of the magnetic part of the amplitude and the error of the combination $(N_{16}^r - N_{17})$ will not make it easier to extract a reasonable value, but hopefully new results from KTeV should also help to improve the predictive power of this analysis.

Whereas the analysis summarized so far was based on conservative assumptions, I also speculated about extracting values for N_{14}^r, N_{15}^r, N_{16}^r and N_{17}. Referring to the FMV, the parameters of the model were estimated using the available data and the extracted value of $(N_{16}^r - N_{17})$. The central values of these parameters were further used to estimate the central values of these four low-energy couplings and to give a prediction about the K^+ decay width without any free parameter. Although the errors are big, the obtained values for the LECs seem to be reasonable.

Acknowledgements

Most of this work was done in Vienna and I would like to thank G. Ecker for his help through a long time. I thank G. Isidori, G. D'Ambrosio and R. Escribano because of helpful discussions on physics and computing. I am grateful for important comments on the experimental input by T. Barker, B. Cox and S. Ledovskoy from the KTeV collaboration. Finally, G. Pancheri should be mentioned since she made it possible for me to come to the LNF in Frascati.

A Loop functions

All loop integrals in this calculation can be reduced to a basis of three scalar integrals:

$$\begin{aligned} iA(m^2) &= \int \frac{d^dk}{(2\pi)^d}\frac{1}{D_1}, \\ iB(q^2,m^2,M^2) &= \int \frac{d^dk}{(2\pi)^d}\frac{1}{D_2}, \\ iC(q^2,p^2,m^2,M^2) &= \int \frac{d^dk}{(2\pi)^d}\frac{1}{D_3}, \end{aligned} \tag{44}$$

with the abbreviations $D_1 = [k^2 - m^2]$, $D_2 = [k^2 - m^2][(k-q)^2 - M^2]$ and $D_3 = [k^2 - m^2][(k-q)^2 - M^2][(k-p)^2 - M^2]$. Indexed loop functions (which can be given explicitly in terms of (44)) are defined through the following relations:

$$\begin{aligned}
\int \frac{d^dk}{(2\pi)^d}\frac{k_\mu}{D_2} &= iq_\mu B_1(q^2,m^2,M^2), \qquad (45)\\
\int \frac{d^dk}{(2\pi)^d}\frac{k_\mu}{D_3} &= iq_\mu C_1(q^2,p^2,qp,m^2,M^2) + ip_\mu C_2(q^2,p^2,qp,m^2,M^2),\\
\int \frac{d^dk}{(2\pi)^d}\frac{k_\mu k_\nu}{D_2} &= ig_{\mu\nu} B_{00}(q^2,m^2,M^2) + iq_\mu q_\nu B_{11}(q^2,m^2,M^2),\\
\int \frac{d^dk}{(2\pi)^2}\frac{k_\mu k_\nu}{D_3} &= ig_{\mu\nu} C_{00}(q^2,p^2,qp,m^2,M^2) + iq_\mu q_\nu C_{11}(q^2,p^2,qp,m^2,M^2)\\
&\quad +i(q_\mu p_\nu + q_\nu p_\mu)C_{12}(q^2,p^2,qp,m^2,M^2) + ip_\mu p_\nu C_{22}(q^2,p^2,qp,m^2,M^2).
\end{aligned}$$

Divergences arise through the loop functions A and B. The divergent parts of these functions are isolated in expressions similar to (9).

$$\begin{aligned}
A(m^2)|_{div} &= -\frac{2m^2\mu^{d-4}}{16\pi^2}\Big\{\frac{1}{d-4} - \frac{1}{2}(\ln 4\pi + 1 - \gamma_E)\Big\},\\
B(q^2,m^2,M^2)|_{div} &= -\frac{2\mu^{d-4}}{16\pi^2}\Big\{\frac{1}{d-4} - \frac{1}{2}(\ln 4\pi + 1 - \gamma_E)\Big\}. \qquad (46)
\end{aligned}$$

All C like functions are finite except C_{00}.

B $K_L \to \pi^+\pi^-\gamma^\star$ form factor $\mathcal{F}_{16}^{Ll}$

Topologies 2 and 3 produce the following contributions; the first part is due to the loop particles (K_1^0, π^-), the second arises from (K^-, η_8), and the very last line comes from (K^-, π^0). Sometimes the Gell-Mann-Okubo mass relation was used to simplify the expressions.

$$\begin{aligned}
\mathcal{F}_{16}^{Ll} &= \frac{-ieG_8}{F}\cdot\Big\{ -2A(m_\pi^2) - \frac{1}{2}(q^2+2qp_1)B(q^2,m_\pi^2,m_\pi^2) + \frac{1}{2(q^2+2qp_1)}\cdot\\
&\Big[2m_\pi^2(q^2+2qp_1-m_K^2) + m_K^2(m_K^2-q^2-2qp_1)\Big]\Big(B(m_\pi^2,m_K^2,m_\pi^2)\\
&-B((p_1+q)^2,m_K^2,m_\pi^2)\Big) + \frac{1}{q^2+2qp_1}\Big[m_K^2(m_\pi^2+p_1p_2+qp_2-q^2\\
&-2qp_1) - 2m_\pi^2(p_1p_2+qp_2)\Big]B_1(m_\pi^2,m_K^2,m_\pi^2)\frac{1}{2(q^2+2qp_1)}\Big[m_K^2(-2m_\pi^2\\
&-q^2-2qp_1-2p_1p_2-2qp_2) + m_\pi^2(2q^2+4qp_1+4p_1p_2+4qp_2) + 2q^4
\end{aligned}$$

$$+q^2(8qp_1+2p_1p_2+2qp_2)+8qp_1^2+4p_1p_2qp_1+4qp_2qp_1\Big]$$
$$B_1((p_1+q)^2,m_K^2,m_\pi^2)+4B_{00}(q^2,m_\pi^2,m_\pi^2)+\frac{2(p_1p_2+qp_2)}{q^2+2qp_1}$$
$$\Big[B_{00}(m_\pi^2,m_K^2,m_\pi^2)-B_{00}((p_1+q)^2,m_K^2,m_\pi^2)+m_\pi^2B_{11}(m_\pi^2,m_K^2,m_\pi^2)$$
$$-(m_\pi^2+q^2+2qp_1)B_{11}((p_1+q)^2,m_K^2,m_\pi^2)\Big]-\frac{1}{2}\Big[m_K^2(m_K^2-q^2-2qp_1$$
$$-2m_\pi^2)+2m_\pi^2(q^2+2qp_1)\Big]C(m_\pi^2,(p_1+q)^2,m_K^2,m_\pi^2)+\frac{1}{2}\Big[m_K^2(-4p_1p_2$$
$$-4m_\pi^2+m_K^2-2q^2-4qp_1)+m_\pi^2(4p_1p_2+4q^2+8qp_1)\Big]$$
$$C_1(m_\pi^2,(p_1+q)^2,m_K^2,m_\pi^2)+\frac{1}{2}\Big[m_K^2(-4m_\pi^2-6qp_1-4p_1p_2-4qp_2+m_K^2$$
$$-2q^2)+4m_\pi^2(q^2+2qp_1+p_1p_2+qp_2)+2qp_1(q^2+2qp_1)\Big]$$
$$C_2(m_\pi^2,(p_1+q)^2,m_K^2,m_\pi^2)+m_K^2C_{00}(m_\pi^2,(p_1+q)^2,m_K^2,m_\pi^2)-2(m_\pi^2$$
$$-m_K^2)C_{00}(m_\pi^2,(p_2+q)^2,m_K^2,m_\pi^2)+(2m_K^2p_1p_2+m_K^2m_\pi^2-2m_\pi^2p_1p_2)$$
$$C_{11}(m_\pi^2,(p_1+q)^2,m_K^2,m_\pi^2)+\Big[m_K^2(qp_1+2qp_2+2m_\pi^2+4p_1p_2)-2m_\pi^2(qp_2$$
$$+2p_1p_2)\Big]C_{12}(m_\pi^2,(p_1+q)^2,m_K^2,m_\pi^2)+\Big[m_K^2(2p_1p_2+2qp_2+m_\pi^2+qp_1)$$
$$-2m_\pi^2(p_1p_2+qp_2)\Big]C_{22}(m_\pi^2,(p_1+q)^2,m_K^2,m_\pi^2)$$

$$-\frac{11}{6}A(m_K^2)-\frac{1}{9}\Big[m_\pi^2+2m_K^2+6(2qp_1+qp_2+p_1p_2+q^2)\Big]B(q^2,m_K^2,m_K^2)$$
$$+\frac{1}{18(q^2+2qp_1)}\Big[m_\eta^2\Big(-6(p_1p_2+qp_2+q^2+2qp_1)+2m_K^2-11m_\pi^2\Big)+3m_\pi^2$$
$$(m_\pi^2+6q^2+12qp_1+2m_K^2+6p_1p_2+6qp_2)\Big]\Big(B(m_\pi^2,m_\eta^2,m_K^2)$$
$$-B((p_1+q)^2,m_\eta^2,m_K^2)\Big)+\frac{1}{9(q^2+2qp_1)}\Big[9m_\eta^2(m_\pi^2+p_1p_2+qp_2-q^2-2qp_1)$$
$$+m_\pi^2(-11m_\pi^2-9q^2-18qp_1-4m_K^2-39p_1p_2-39qp_2)+6m_K^2(q^2+2qp_1)\Big]$$
$$B_1(m_\pi^2,m_\eta^2,m_K^2)-\frac{1}{9(q^2+2qp_1)}\Big[3m_\eta^2(2q^2+4qp_1+3p_1p_2+3qp_2+3m_\pi^2)$$
$$+m_\pi^2(-11m_\pi^2-4m_K^2-29q^2-58qp_1-39p_1p_2-39qp_2)-4m_K^2(q^2+2qp_1)$$
$$-72qp_1^2-72q^2qp_1-18q^4-30q^2p_1p_2-30q^2qp_2-60qp_1p_1p_2-60qp_1qp_2\Big]$$
$$B_1((p_1+q)^2,m_\eta^2,m_K^2)+5B_{00}(q^2,m_K^2,m_K^2)+\frac{4}{3(q^2+2qp_1)}\Big[(m_\pi^2+3p_1p_2$$
$$+3qp_2)B_{00}(m_\pi^2,m_\eta^2,m_K^2)-(m_\pi^2+q^2+2qp_1+3p_1p_2+3qp_2)$$

$$
\begin{aligned}
&B_{00}((p_1+q)^2,m_\eta^2,m_K^2)\Big] + \frac{4}{3(q^2+2qp_1)}\Big[m_\pi^2(m_\pi^2+3p_1p_2+3qp_2)\\
&B_{11}(m_\pi^2,m_\eta^2,m_K^2) - \Big(m_\pi^2(m_\pi^2+2q^2+4qp_1+3p_1p_2+3qp_2)+q^2(q^2+4qp_1\\
&+3p_1p_2+3qp_2)+4qp_1^2+6qp_1(qp_2+p_1p_2)\Big)B_{11}((p_1+q)^2,m_\eta^2,m_K^2)\Big]\\
&-\frac{1}{18}\Big[m_\eta^2\Big(-6(p_1p_2+q^2+2qp_1+qp_2)-11m_\pi^2+2m_K^2\Big)+3m_\pi^2(6p_1p_2\\
&+6qp_2+6q^2+12qp_1+m_\pi^2+2m_K^2)\Big]C(m_\pi^2,(p_1+q)^2,m_\eta^2,m_K^2)+\frac{1}{18}\Big[3m_\eta^2\\
&(-14m_\pi^2-24p_1p_2-18qp_1-6qp_2-6q^2-2m_K^2+m_\eta^2)+m_\pi^2(24m_K^2\\
&+30qp_2+66qp_1+48p_1p_2+30q^2+11m_\pi^2)+m_K^2(36qp_1+12qp_2+12q^2\\
&+48p_1p_2+4m_K^2)\Big]C_1(m_\pi^2,(p_1+q)^2,m_\eta^2,m_K^2)+\frac{1}{18}\Big[3m_\eta^2(m_\eta^2-2m_K^2\\
&-14m_\pi^2-12q^2-28qp_1-24qp_2-24p_1p_2)+m_\pi^2(11m_\pi^2+24m_K^2+36q^2\\
&+76qp_1+48qp_2+48p_1p_2)+4m_K^2(6q^2+14qp_1+12qp_2+12p_1p_2+m_K^2)\\
&+24qp_1(q^2+qp_2+p_1p_2+2qp_1)\Big]C_2(m_\pi^2,(p_1+q)^2,m_\eta^2,m_K^2)+2(m_K^2-m_\pi^2)\\
&C_{00}(m_\pi^2,(p_2+q)^2,m_\eta^2,m_K^2)+\frac{2}{3}(m_\eta^2+m_K^2-m_\pi^2)C_{00}(m_\pi^2,(p_1+q)^2,m_\eta^2,m_K^2)\\
&+\frac{1}{3}\Big[m_\eta^2(5m_\pi^2+3qp_1+9p_1p_2)-m_\pi^2(m_\pi^2+2m_K^2+qp_1+3p_1p_2)-2m_K^2\\
&(qp_1+3p_1p_2)\Big]C_{11}(m_\pi^2,(p_1+q)^2,m_\eta^2,m_K^2)+\frac{1}{3}\Big[m_\eta^2(10m_\pi^2+3q^2+11qp_1\\
&+9qp_2+18p_1p_2)-m_\pi^2(2m_\pi^2+4m_K^2+q^2+3qp_1+3qp_2+6p_1p_2)-2m_K^2(q^2\\
&+3qp_1+3qp_2+6p_1p_2)\Big]C_{12}(m_\pi^2,(p_1+q)^2,m_\eta^2,m_K^2)+\frac{1}{3}\Big[m_\eta^2(5m_\pi^2+3q^2\\
&+8qp_1+9qp_2+9p_1p_2)-m_\pi^2(m_\pi^2+2m_K^2+q^2+2qp_1+3qp_2+3p_1p_2)\\
&-2m_K^2(q^2+2qp_1+3qp_2+3p_1p_2)\Big]C_{22}(m_\pi^2,(p_1+q)^2,m_\eta^2,m_K^2)\\
&+\frac{(d-2)}{2(d-1)}A(m_K^2)+\frac{1}{4(d-1)}B(q^2,m_K^2,m_K^2)(q^2-4m_K^2)\Big\}. \qquad (47)
\end{aligned}
$$

C $K^+ \to \pi^+\pi^0\gamma^\star$ form factors $\mathcal{F}^{+l}_{15,16}$ and $\mathcal{F}^{+l}_{25,26}$

They are split up into two pieces, where I distinguish between contributions with an η_8 in the loop and contributions with a pair of any kaon and pion. The η_8 parts read as:

$$
\begin{aligned}
\mathcal{F}^{+l}_{15} \;=\; &\frac{-ieG_8}{F}\cdot\Big\{-\frac{1}{9(q^2+2qp_1)(q^2+2qp_1+2qp_2)}\Big[m_\pi^2(6q^2+12qp_1+22qp_2)
\end{aligned}
$$

$$+m_K^2(-3q^2-6qp_1-qp_2)+6q^2(q^2+4qp_1+4qp_2+p_1p_2)+12qp_1(2qp_1$$
$$+4qp_2+p_1p_2)+24qp_2(qp_2+p_1p_2)\Big]A(m_K^2)+\frac{1}{18(q^2+2qp_1)(q^2+2qp_1+2qp_2)}$$
$$\Big[3m_\eta^2(-2m_\pi^2+m_K^2-q^2-2qp_1-2p_1p_2)+m_\pi^2(26m_\pi^2-15m_K^2+13q^2$$
$$+26qp_1+12qp_2+38p_1p_2)+m_K^2(m_K^2-q^2-2qp_1-6qp_2-8p_1p_2)+6p_1p_2$$
$$(q^2+2qp_1+2qp_2+2p_1p_2)\Big]A(m_\eta^2)+\frac{1}{9}(11m_\pi^2-8m_K^2+6qp_2+6p_1p_2)$$
$$B(q^2,m_K^2,m_K^2)+\frac{1}{54(q^2+2qp_1)(q^2+2qp_1+2qp_2)}\Big[m_\pi^2m_K^2(-12m_\pi^2+24m_K^2$$
$$-58q^2-116qp_1-60p_1p_2)+m_\pi^2p_1p_2(-12q^2-24qp_1-240m_\pi^2-144p_1p_2$$
$$-144qp_2)+m_K^2p_1p_2(30m_K^2-60q^2-120qp_1-72qp_2-72p_1p_2)+m_\pi^4$$
$$(-28q^2-56qp_1-144qp_2)+m_K^4(5q^2+10qp_1+36qp_2)+m_\pi^2(60q^4+240qp_1^2$$
$$+240q^2qp_1+120q^2qp_2+240qp_1qp_2)+m_K^2(-24q^4-96qp_1^2-96q^2qp_1$$
$$-48q^2qp_2-96qp_1qp_2)+3m_K^6-96m_\pi^6\Big]B(m_\pi^2,m_\eta^2,m_K^2)+\frac{1}{18(q^2+2qp_1)}$$
$$\Big[m_\eta^2(-3m_\eta^2+8m_K^2-2m_\pi^2-6qp_2-6p_1p_2)+m_\pi^2(33m_\pi^2-24m_K^2+18qp_2$$
$$+18p_1p_2)\Big]B((p_1+q)^2,m_\eta^2,m_K^2)-\frac{1}{18(q^2+2qp_1+2qp_2)}\Big[9m_\eta^2(-2m_\pi^2-q^2$$
$$-2qp_1-2qp_2-2p_1p_2)+m_\pi^2(22m_\pi^2+8m_K^2+27q^2+54qp_1+54qp_2$$
$$+78p_1p_2)+6m_K^2(q^2+2qp_1+2qp_2)\Big]B_1(m_\pi^2,m_\eta^2,m_K^2)$$
$$+\frac{1}{(q^2+2qp_1)(q^2+2qp_1+2qp_2)}\Big[m_\pi^2m_K^2(-2m_\pi^2-m_K^2+q^2+2qp_1-4qp_2$$
$$-2p_1p_2)+m_\pi^2p_1p_2(20m_\pi^2+6q^2+12qp_1+12qp_2+12p_1p_2)+m_K^2p_1p_2$$
$$(-m_K^2+q^2+2qp_1+2qp_2+2p_1p_2)+4m^4(q^2+2qp_1+3qp_2+2m_\pi^2)-m_K^4qp_2\Big]$$
$$B_1(m_\pi^2,m_K^2,m_\eta^2)+\frac{1}{9(q^2+2qp_1)}\Big[m_\pi^2(-10m_\pi^2+4m_K^2-5q^2-10qp_1+18qp_2$$
$$+18p_1p_2)+4m_K^2(2q^2+4qp_1-3qp_2-3p_1p_2)+6q^2(q^2+4qp_1+qp_2$$
$$+p_1p_2)+12qp_1(2qp_1+qp_2+p_1p_2)\Big]B_1((p_1+q)^2,m_\eta^2,m_K^2)$$
$$+2B_{00}(q^2,m_K^2,m_K^2)+\frac{4(m_\pi^2+3p_1p_2)}{3(q^2+2qp_1+2qp_2)}B_{00}(m_\pi^2,m_\eta^2,m_K^2)$$
$$-\frac{2}{(q^2+2qp_1)(q^2+2qp_1+2qp_2)}\Big[2m_\pi^2(2m_\pi^2-m_K^2+q^2+2qp_1+3qp_2$$
$$+5p_1p_2)-3m_K^2(qp_2+p_1p_2)+3p_1p_2(q^2+2qp_1+2qp_2+2p_1p_2)\Big]$$

$$
\begin{aligned}
&B_{00}(m_\pi^2,m_K^2,m_\eta^2)-\frac{2}{3(q^2+2qp_1)}\Big[2m_\pi^2+6qp_2+6p_1p_2+2q^2+4qp_1\Big]\\
&B_{00}((p_1+q)^2,m_\eta^2,m_K^2)+\frac{4m_\pi^2(m_\pi^2+3p_1p_2)}{3(q^2+2qp_1+2qp_2)}B_{11}(m_\pi^2,m_\eta^2,m_K^2)\\
&-\frac{2m_\pi^2}{(q^2+2qp_1)(q^2+2qp_1+2qp_2)}\Big[2m_\pi^2(2m_\pi^2-m_K^2+q^2+2qp_1+3qp_2\\
&+5p_1p_2)-3m_K^2(qp_2+p_1p_2)+3p_1p_2(q^2+2qp_1+2qp_2+2p_1p_2)\Big]\\
&B_{11}(m_\pi^2,m_K^2,m_\eta^2)-\frac{4}{3(q^2+2qp_1)}\Big[m_\pi^2(m_\pi^2+2q^2+4qp_1+3qp_2+3p_1p_2)\\
&+q^2(q^2+4qp_1+3qp_2+3p_1p_2)+qp_1(4qp_1+6qp_2+6p_1p_2)\Big]\\
&B_{11}((p_1+q)^2,m_\eta^2,m_K^2)+\frac{1}{18}\Big[\Big(m_\eta^2(-3m_\eta^2-2m_\pi^2+8m_K^2-6qp_2-6p_1p_2)\\
&+m_\pi^2(33m_\pi^2-24m_K^2+18qp_2+18p_1p_2)\Big)C(m_\pi^2,(p_1+q)^2,m_\eta^2,m_K^2)\\
&-\Big(m_\eta^2(-3m_\eta^2+6m_\pi^2+24m_K^2+18qp_1-18qp_2+36p_1p_2)+m_\pi^2(49m_\pi^2\\
&-30m_K^2-6qp_1+30qp_2+12p_1p_2)+m_K^2(-16m_K^2-12qp_1+12qp_2\\
&-24p_1p_2)\Big)C_1(m_\pi^2,(p_1+q)^2,m_\eta^2,m_K^2)-\Big(m_\eta^2(-3m_\eta^2+6m_\pi^2+24m_K^2\\
&+18q^2+48qp_1+36qp_2+36p_1p_2)+m_\pi^2(49m_\pi^2-30m_K^2-6q^2+32qp_1\\
&+12qp_2+12p_1p_2)+m_K^2(-16m_K^2-12q^2-56qp_1-24qp_2-24p_1p_2)\\
&+24qp_1qp_2+24qp_1p_1p_2\Big)C_2(m_\pi^2,(p_1+q)^2,m_\eta^2,m_K^2)\Big]-\frac{1}{3}\Big[(-5m_\eta^2+m_\pi^2\\
&+2m_K^2)C_{00}(m_\pi^2,(p_1+q)^2,m_\eta^2,m_K^2)+\Big(m_\eta^2(-5m_\pi^2-3qp_1-9p_1p_2)+m_\pi^2\\
&(m_\pi^2+2m_K^2+qp_1+3p_1p_2)+m_K^2(2qp_1+6p_1p_2)\Big)\\
&C_{11}(m_\pi^2,(p_1+q)^2,m_\eta^2,m_K^2)+\Big(m_\eta^2(-5m_\pi^2-3q^2-8qp_1-9qp_2-9p_1p_2)\\
&+m_\pi^2(m_\pi^2+2m_K^2+q^2+2qp_1+3qp_2+3p_1p_2)+m_K^2(2q^2+4qp_1+6qp_2\\
&+6p_1p_2)\Big)C_{22}(m_\pi^2,(p_1+q)^2,m_\eta^2,m_K^2)+\Big(m_\eta^2(-10m_\pi^2-3q^2-11qp_1\\
&-9qp_2-18p_1p_2)+m_\pi^2(2m_\pi^2+4m_K^2+q^2+3qp_1+3qp_2+6p_1p_2)\\
&+m_K^2(2q^2+6qp_1+6qp_2+12p_1p_2)\Big)C_{12}(m_\pi^2,(p_1+q)^2,m_\eta^2,m_K^2)\Big]\Big\},
\end{aligned}
\tag{48}
$$

$$
\begin{aligned}
\mathcal{F}_{25}^{+l} &= \frac{-ieG_8}{F}\cdot\Big\{\frac{1}{18(q^2+2qp_1+2qp_2)}(-3q^2-6qp_1-6qp_2+12p_1p_2+5m_K^2\\
&+10m_\pi^2)A(m_K^2)+\frac{1}{18(q^2+2qp_1+2qp_2)}(54p_1p_2+62m_\pi^2-29m_K^2)A(m_\eta^2)
\end{aligned}
$$

$$
-\frac{1}{54(q^2+2qp_1+2qp_2)}\Big[m_\pi^2(-30q^2-60qp_1-60qp_2-60p_1p_2-44m_\pi^2
$$
$$
+58m_K^2)+m_K^2(12q^2+24qp_1+24qp_2+24p_1p_2+13m_K^2)\Big]B(m_\pi^2,m_\eta^2,m_K^2)
$$
$$
-\frac{1}{9(q^2+2qp_1+2qp_2)}\Big[m_\pi^2(6q^2+12qp_1+12qp_2+39p_1p_2+11m_\pi^2+4m_K^2
$$
$$
-9m_\eta^2)-9p_1p_2m_\eta^2\Big]B_1(m_\pi^2,m_\eta^2,m_K^2)+\frac{1}{2(q^2+2qp_1+2qp_2)}\Big[m_\pi^2(2m_\pi^2
$$
$$
+6p_1p_2+9m_K^2-6m_\eta^2)+m_K^2(-2m_K^2+6p_1p_2+3m_\eta^2)-6p_1p_2m_\eta^2\Big]
$$
$$
B_1(m_\pi^2,m_K^2,m_\eta^2)+3B_{00}(q^2,m_K^2,m_K^2)-2B_{00}((p_1+q)^2,m_\eta^2,m_K^2)
$$
$$
+\frac{4(m_\pi^2+3p_1p_2)}{3(q^2+2qp_1+2qp_2)}B_{00}(m_\pi^2,m_\eta^2,m_K^2)+2B_{00}((p_1+q)^2,m_\eta^2,m_K^2)
$$
$$
-\frac{2(2m_\pi^2+3p_1p_2)}{q^2+2qp_1+2qp_2}B_{00}(m_\pi^2,m_K^2,m_\eta^2)+\frac{4m_\pi^2(m_\pi^2+3p_1p_2)}{3(q^2+2qp_1+2qp_2)}
$$
$$
B_{11}(m_\pi^2,m_\eta^2,m_K^2)-\frac{2m_\pi^2(2m_\pi^2+3p_1p_2)}{q^2+2qp_1+2qp_2}B_{11}(m_\pi^2,m_K^2,m_\eta^2)+2(m_K^2-m_\pi^2)
$$
$$
C_{00}(m_\pi^2,(p_1+q)^2,m_\eta^2,m_K^2)\Big\}. \qquad (49)
$$

The different contributions of the (K,π) pairs are collected in the form factors $\mathcal{F}_{16}^{+l}$ and $\mathcal{F}_{26}^{+l}$. The first lines refer to (K^0,π^0), then follow (K^-,π^0), (K^0,π^-) and (K^+,π^-).

$$
\begin{aligned}
\mathcal{F}_{16}^{+l} \;=\; & \frac{-ieG_8}{F}\Big\{\frac{1}{(q^2+2qp_1)(q^2+2qp_1+2qp_2)}\Big[-\frac{1}{2}\Big(2m_\pi^2(2m_\pi^2+q^2+2qp_1 \\
& +2qp_2+4p_1p_2)+m_K^2(-m_K^2+q^2+2qp_1-2qp_2)+2p_1p_2(q^2 \\
& +2qp_1+2qp_2+2p_1p_2)\Big)A(m_\pi^2)+\frac{m_K^2}{2}\Big(2m_\pi^2(2m_\pi^2-2m_K^2 \\
& +q^2+2qp_1+2p_1p_2)+m_K^2(m_K^2-q^2-2qp_1-2p_1p_2)\Big) \\
& B(m_\pi^2,m_K^2,m_\pi^2)-\Big(m_\pi^2m_K^2(-m_K^2+2m_\pi^2+q^2+2qp_1+4qp_2+6p_1p_2) \\
& -2m_\pi^2p_1p_2(2m_\pi^2+q^2+2qp_1+2qp_2+2p_1p_2)+m_K^2p_1p_2(-m_K^2+q^2 \\
& +2qp_1+2qp_2+2p_1p_2)-4m_\pi^4qp_2-m_K^4qp_2\Big)B_1(m_\pi^2,m_K^2,m_\pi^2) \\
& -2\Big(p_1p_2(2m_\pi^2-m_K^2+q^2+2qp_1+2qp_2+2p_1p_2)+2m_\pi^2qp_2-m_K^2qp_2\Big) \\
& \Big(B_{00}(m_\pi^2,m_K^2,m_\pi^2)+m_\pi^2B_{11}(m_\pi^2,m_K^2,m_\pi^2)\Big)\Big] \\
& +\frac{1}{3(q^2+2qp_1)(q^2+2qp_1+2qp_2)}\Big[2m_\pi^2(q^2+2qp_1+4qp_2)+m_K^2
\end{aligned}
$$

$$(-q^2-2qp_1+qp_2)+2q^2(q^2+4qp_1+4qp_2+p_1p_2)+4p_1p_2(qp_1$$
$$+2qp_2)+8(qp_1^2+qp_2^2+2qp_1qp_2)\Big]A(m_K^2)-\frac{1}{3(d-1)}$$
$$A(m_K^2)+\frac{1}{6(d-1)}\Big(q^2-4m_K^2\Big)B(q^2,m_K^2,m_K^2)$$
$$-\frac{1}{(q^2+2qp_1)(q^2+2qp_1+2qp_2)}\Big[2m_\pi^2(q^2+2qp_1+3qp_2)-m_K^2(q^2$$
$$+2qp_1)+2q^2(q^2+4qp_1+4qp_2+p_1p_2)+4p_1p_2(qp_1+2qp_2)+8(qp_1^2$$
$$+qp_2^2+2qp_1qp_2)\Big]A(m_\pi^2)+\frac{1}{q^2+2qp_1+2qp_2}\Big[-\Big(q^2(m_K^2-m_\pi^2)$$
$$-m_K^4+m_\pi^2m_K^2-2m_\pi^2(qp_1+qp_2)+2m_K^2(qp_1+qp_2)\Big)B(m_\pi^2,m_K^2,m_\pi^2)$$
$$+2p_1p_2(m_K^2-m_\pi^2)B_1(m_\pi^2,m_K^2,m_\pi^2)\Big]-\frac{1}{q^2+2qp_1}\Big[\Big(-2m_\pi^4+2m_\pi^2m_K^2$$
$$-2m_\pi^2(qp_2+p_1p_2)+2m_K^2(qp_2+p_1p_2)\Big)B((p_1+q)^2,m_K^2,m_\pi^2)$$
$$+2(m_K^2-m_\pi^2)(qp_2+p_1p_2)B_1((p_1+q)^2,m_K^2,m_\pi^2)\Big]$$
$$+2B_{00}(q^2,m_\pi^2,m_\pi^2)+\Big[2m_\pi^2(m_\pi^2-m_K^2+qp_2+p_1p_2)-2m_K^2(qp_2$$
$$+p_1p_2)\Big]C(m_\pi^2,(p_1+q)^2,m_K^2,m_\pi^2)-\Big[2m_\pi^2(m_\pi^2-m_K^2+qp_2)$$
$$-2m_K^2qp_2\Big]C_1(m_\pi^2,(p_1+q)^2,m_K^2,m_\pi^2)-2m_\pi^2\Big(m_\pi^2-m_K^2\Big)$$
$$C_2(m_\pi^2,(p_1+q)^2,m_K^2,m_\pi^2)-2p_1p_2(m_\pi^2-m_K^2)$$
$$C_{11}(m_\pi^2,(p_1+q)^2,m_K^2,m_\pi^2)-2(m_\pi^2-m_K^2)(qp_2+p_1p_2)$$
$$C_{22}(m_\pi^2,(p_1+q)^2,m_K^2,m_\pi^2)-2(m_\pi^2-m_K^2)(qp_2+2p_1p_2)$$
$$C_{12}(m_\pi^2,(p_1+q)^2,m_K^2,m_\pi^2)$$
$$+\frac{1}{3(q^2+2qp_1)(q^2+2qp_1+2qp_2)}\Big[-\Big(2m_\pi^2(4m_\pi^2-4m_K^2-q^2-2qp_1$$
$$+8qp_2+12p_1p_2)+m_K^2(2m_K^2+q^2+2qp_1-8qp_2-12p_1p_2)+2p_1p_2$$
$$(q^2+2qp_1+8qp_2+8p_1p_2)\Big)A(m_\pi^2)-m_K^2\Big(2m_\pi^2(2m_\pi^2-3m_K^2-2q^2$$
$$-4qp_1+2qp_2+4p_1p_2)+m_K^2(2m_K^2+q^2+2qp_1-2qp_2-6p_1p_2)$$
$$+4p_1p_2(-q^2-2qp_1+qp_2+p_1p_2)\Big)B(m_\pi^2,m_K^2,m_\pi^2)+2\Big(4m_\pi^6$$
$$+4m_\pi^4(-2m_K^2-q^2-2qp_1+qp_2+2p_1p_2)+3m_K^4(m_\pi^2+qp_2+p_1p_2)$$
$$+2m_\pi^2p_1p_2(-7m_K^2-2q^2-4qp_1+2qp_2+2p_1p_2)-3m_K^2p_1p_2(q^2$$
$$+2qp_1+2qp_2+2p_1p_2)-8m_\pi^2m_K^2qp_2\Big)B_1(m_\pi^2,m_K^2,m_\pi^2)+4\Big(m_\pi^2$$

$$(2m_\pi^2 - m_K^2 + q^2 + 2qp_1 + 6qp_2 + 8p_1p_2) - 3m_K^2(qp_2 + p_1p_2)$$
$$+3p_1p_2(q^2 + 2qp_1 + 2qp_2 + 2p_1p_2)\Big)\Big(B_{00}(m_\pi^2, m_K^2, m_\pi^2) + m_\pi^2$$
$$B_{11}(m_\pi^2, m_K^2, m_\pi)\Big)\Big] + 2B_{00}(q^2, m_K^2, m_K^2)\Big\}. \qquad (50)$$

$\mathcal{F}_{26}^{+l}$ is organized in the same way and reads as follows:

$$\begin{aligned}
\mathcal{F}_{26}^{+l} &= \frac{-ieG_8}{F}\Big\{\frac{1}{q^2 + 2qp_1 + 2qp_2}\Big[\frac{1}{2}(2m_\pi^2 - 3m_K^2 + 2p_1p_2)A(m_\pi^2) + \frac{m_K^2}{2} \\
&(2m_\pi^2 - m_K^2)B(m_\pi^2, m_K^2, m_\pi^2) - (2m_\pi^4 + m_K^4 - 2m_\pi^2 m_K^2 - m_K^2 p_1p_2) \\
&B_1(m_\pi^2, m_K^2, m_\pi^2) - 2p_1p_2\Big(B_{00}(m_\pi^2, m_K^2, m_\pi^2) + m_\pi^2 B_{11}(m_\pi^2, m_K^2, m_\pi^2)\Big)\Big] \\
&+\frac{1}{6(q^2 + 2qp_1 + 2qp_2)}\Big[-4m_\pi^2 - 3m_K^2 + q^2 + 2qp_1 + 2qp_2 - 4p_1p_2\Big] \\
&A(m_K^2) - \frac{1}{2(d-1)}A(m_K^2) + \frac{1}{4(d-1)}(q^2 - 4m_K^2)B(q^2, m_K^2, m_K^2) \\
&+\frac{1}{q^2 + 2qp_1 + 2qp_2}\Big[(m_\pi^2 + m_K^2 + 2p_1p_2)A(m_\pi^2) + m_K^2(m_K^2 - m_\pi^2) \\
&B(m_\pi^2, m_K^2, m_\pi^2) + 2p_1p_2(m_K^2 - m_\pi^2)B_1(m_\pi^2, m_K^2, m_\pi^2)\Big] \\
&+2B_{00}(q^2, m_\pi^2, m_\pi^2) + 2(m_K^2 - m_\pi^2)C_{00}(m_\pi^2, (p_1 + q)^2, m_K^2, m_\pi^2) \\
&+\frac{1}{3(q^2 + 2qp_1 + 2qp_2)}\Big[4(2m_\pi^2 - m_K^2 + p_1p_2)A(m_\pi^2) + 2m_K^2(m_\pi^2 \\
&+p_1p_2)B(m_\pi^2, m_K^2, m_\pi^2) - 2[m_\pi^2(2m_\pi^2 - 3m_K^2 + 2p_1p_2) + m_K^2(2m_K^2 \\
&-p_1p_2)]B_1(m_\pi^2, m_K^2, m_\pi^2)\Big] + \frac{2}{3}\Big[(m_\pi^2 - m_K^2 + qp_1 + p_1p_2) \\
&B((p_2 + q)^2, m_K^2, m_\pi^2) + (m_K^2 + q^2 + 2qp_1 + 2qp_2 + 2p_1p_2) \\
&B_1((p_2 + q)^2, m_K^2, m_\pi^2)\Big] - \frac{4(3m_\pi^2 - 2m_K^2 + p_1p_2)}{3(q^2 + 2qp_1 + 2qp_2)}\Big[B_{00}(m_\pi^2, m_K^2, m_\pi^2) \\
&+m_\pi^2 B_{11}(m_\pi^2, m_K^2, m_\pi^2)\Big] - \frac{1}{3}\Big[(2m_\pi^2 - 3m_K^2 + 2qp_1 + 2p_1p_2) \\
&B(q^2, m_\pi^2, m_\pi^2) + (3m_K^2 + 2q^2 + 4qp_1 + 4qp_2 + 4p_1p_2) \\
&B_1((p_2 + q)^2, m_K^2, m_\pi^2)\Big] - \frac{2}{3}m_K^2(m_\pi^2 - m_K^2 + qp_1 + p_1p_2) \\
&C(m_\pi^2, (p_2 + q)^2, m_K^2, m_\pi^2) + \frac{1}{3}\Big[4m_\pi^2(m_\pi^2 - m_K^2 + qp_1 + p_1p_2) + m_K^4\Big] \\
&C_1(m_\pi^2, (p_2 + q)^2, m_K^2, m_\pi^2) + \frac{1}{3}\Big[4m_\pi^2(m_\pi^2 - m_K^2 + qp_1 + qp_2 + p_1p_2) \\
&+4qp_2(-m_K^2 + qp_1 + p_1p_2) + m_K^4\Big]C_2(m_\pi^2, (p_2 + q)^2, m_K^2, m_\pi^2) - \frac{2}{3}m_K^2
\end{aligned}$$

$$\Big[C_{00}(m_\pi^2,(p_2+q)^2,m_K^2,m_\pi^2)+m_\pi^2 C_{11}(m_\pi^2,(p_2+q)^2,m_K^2,m_\pi^2)$$
$$+(m_\pi^2+qp_2)C_{22}(m_\pi^2,(p_2+q)^2,m_K^2,m_\pi^2)+(2m_\pi^2+qp_2)$$
$$C_{12}(m_\pi^2,(p_2+q)^2,m_K^2,m_\pi^2)\Big]+\frac{2}{3}B_{00}(q^2,m_K^2,m_K^2)\Big\}. \qquad (51)$$

References

[1] L.M. Sehgal and M. Wanninger, Phys. Rev. **D46** (1992) 1035.

[2] P. Heiliger and L.M. Sehgal, Phys. Rev. **D48** (1993) 4146.

[3] J.K. Elwood, M.J. Savage and M.B. Wise, Phys. Rev. **D52** (1995) 5095.

[4] M.J. Savage, hep-ph/9908324.

[5] J. Adams *et al.* (KTeV Collaboration), Phys. Rev. Lett. **80** (1998) 4123.

[6] J. Cogan (NA48 Collaboration), talk given at the International Workshop on CP Violation in K, Tanashi, Tokyo (Japan), December 18-19 1998.

[7] Y. Takeuchi *et al.*, Phys. Lett. **B443** (1998) 409.

[8] J.K. Elwood, M.J. Savage, J.W. Walden and M.B. Wise, Phys. Rev. **D53** (1996) 4078.

[9] A. Alavi-Harati *et al.* (KTeV Collaboration), Phys. Rev. Lett. **84** (2000) 408.

[10] J. Belz (KTeV Collaboration), hep-ex/9903025.

[11] J. van Leusen and L.M. Sehgal, Phys. Rev. Lett. **83** (1999) 4933.

[12] J. van Leusen and L.M. Sehgal, hep-ph/0006336.

[13] T. Barker (KTeV Collaboration), in Proc. of Heavy Flavours 8, Southampton, UK, 1999.

[14] S. Adler *et al.* (E787 Collaboration), hep-ex/0007021.

[15] J. Gasser and H. Leutwyler, Ann. Phys. **158** (1984) 142.

[16] J. Gasser and H. Leutwyler, Nucl. Phys. **B250** (1985) 465.

[17] J. Kambor, J. Missimer and D. Wyler, Phys. Lett. **B261** (1991) 496.

[18] J. Kambor, J. Missimer and D. Wyler, Nucl. Phys. **B346** (1990) 17.

[19] G. Ecker, J. Kambor and D. Wyler, Nucl. Phys. **B394** (1993) 101.

[20] G. Ecker, H. Neufeld and A. Pich, Phys. Lett. **B278** (1992) 337.

[21] G. Ecker, H. Neufeld and A. Pich, Nucl. Phys. **B413** (1994) 321.

[22] E.J. Ramberg *et al.*, Phys. Rev. Lett. **70**, (1993) 2525.

[23] G. Ecker, A. Pich and E. de Rafael, Nucl. Phys. **B291** (1987) 692.

[24] C. Alliegro *et al.*, Phys. Rev. Lett. **68** (1992) 278.

[25] G. D'Ambrosio, G. Ecker, G. Isidori and J. Portolés, JHEP **8** (1998) 4.

[26] R. Appel *et al.*, (E865 Collaboration), Phys. Rev. Lett. **83** (1999) 4482.

[27] S.D. Ellis, R. Kleiss and W.J. Stirling, Comp. Phys. Comm. **40** (1986) 359.

[28] C. Bruno and J. Prades, Z. Phys. **C57** (1993) 585.

[29] G. D'Ambrosio and J. Portolés, Nucl. Phys. **B492** (1997) 417.